

The ISA detector test facility

P. Yamin

July 1979

Collider Accelerator Department
Brookhaven National Laboratory

U.S. Department of Energy

USDOE Office of Science (SC)

Notice: This technical note has been authored by employees of Brookhaven Science Associates, LLC under Contract No.DE-AC02-76CH00016 with the U.S. Department of Energy. The publisher by accepting the technical note for publication acknowledges that the United States Government retains a non-exclusive, paid-up, irrevocable, world-wide license to publish or reproduce the published form of this technical note, or allow others to do so, for United States Government purposes.

DISCLAIMER

This report was prepared as an account of work sponsored by an agency of the United States Government. Neither the United States Government nor any agency thereof, nor any of their employees, nor any of their contractors, subcontractors, or their employees, makes any warranty, express or implied, or assumes any legal liability or responsibility for the accuracy, completeness, or any third party's use or the results of such use of any information, apparatus, product, or process disclosed, or represents that its use would not infringe privately owned rights. Reference herein to any specific commercial product, process, or service by trade name, trademark, manufacturer, or otherwise, does not necessarily constitute or imply its endorsement, recommendation, or favoring by the United States Government or any agency thereof or its contractors or subcontractors. The views and opinions of authors expressed herein do not necessarily state or reflect those of the United States Government or any agency thereof.

Accelerator Department
BROOKHAVEN NATIONAL LABORATORY
Associated Universities, Inc.

EP&S DIVISION TECHNICAL NOTE

No. 88

P. Yamin

July 20, 1979

THE ISA DETECTOR TEST FACILITY

A facility for testing detectors to be used at ISABELLE will be constructed at the AGS. During the fall of 1979 the MESB/B4 will be used temporarily, but in early 1980 the B1 line will become available. There are no other commitments or pending proposals for the B1 beam, so it can be devoted to the Detector Test Facility (DTF) indefinitely. As both B1 and B4 service adjacent areas on the AGS floor, a compact layout encompassing both beams is envisioned for late 1981. This is illustrated in Figure 1.

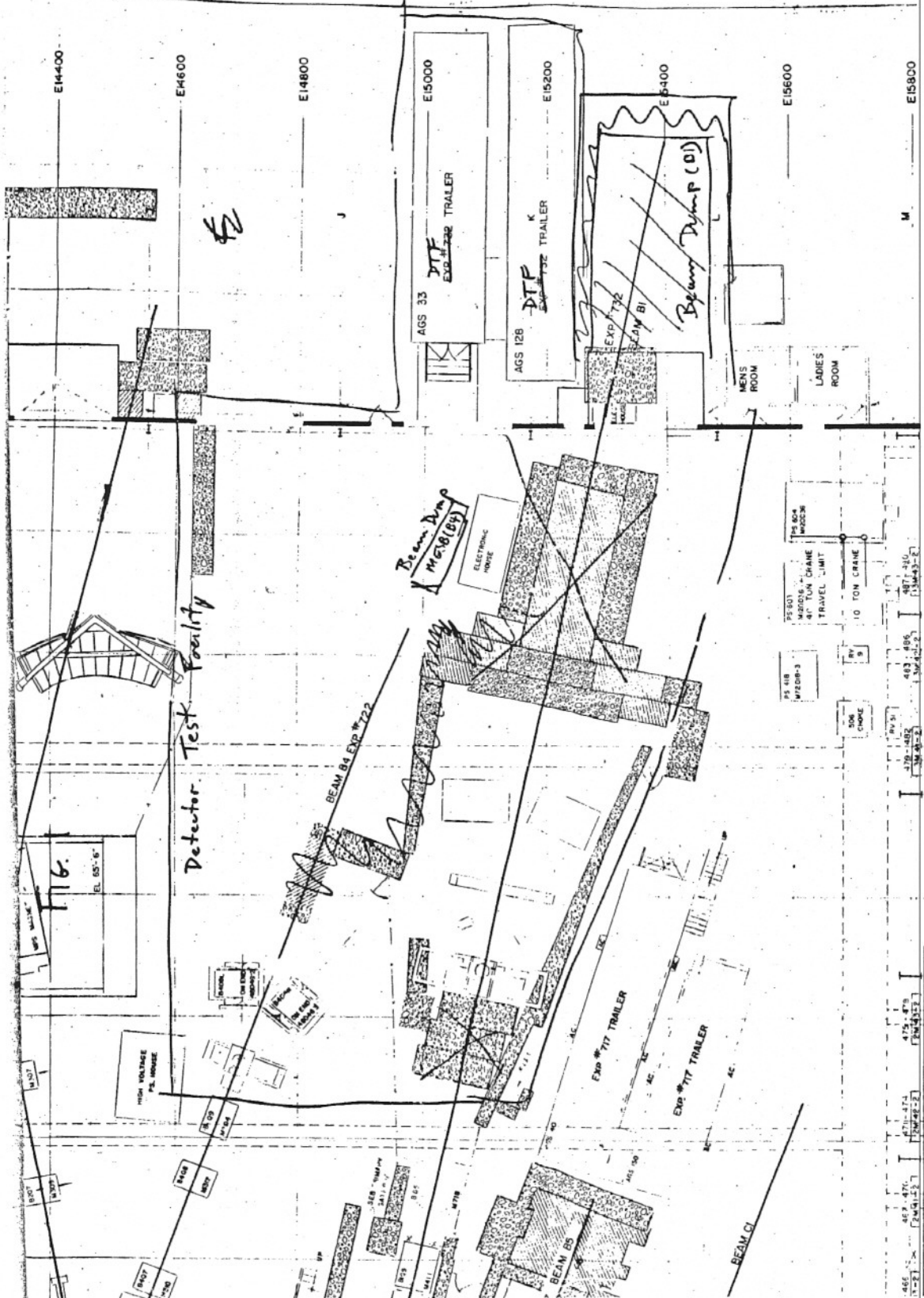
The MESB/B4 provides separated π s, Ks, ps, and \bar{p} s at moderate intensities between 1 and 10 GeV/c. B1 is an unseparated 0° production-angle beam which can deliver high fluxes ($\sim 10^7$ /sec) up to 24 GeV/c. Thus, the DTF will be able to simulate many of the features of the ISABELLE environment. Fig. 2(a-f) shows the particle fluxes available in these beams.

The DTF will be arranged so that tests can be conducted expeditiously. A counting house-trailer will contain a PDP11/60 and will be supplied with NIM and CAMAC electronics from HEEP. Crane coverage is unobstructed, and the area is free of encumbrances. Sufficient water and power will be provided to operate one large spectrometer magnet, and provision will be made for the eventual installation of cryogenic services, should it prove necessary.

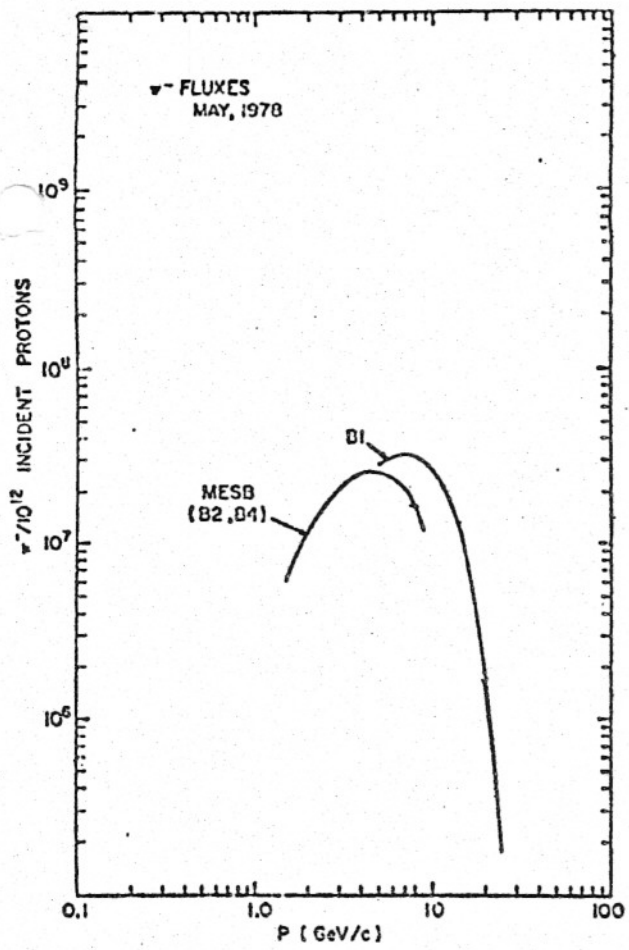
Operating instructions and other details are given in the appendices. Appendix I is a report by C.T. Murphy and J. Fox describing the MESB and Appendix II gives more information about B1 than is available elsewhere.

List of Figures

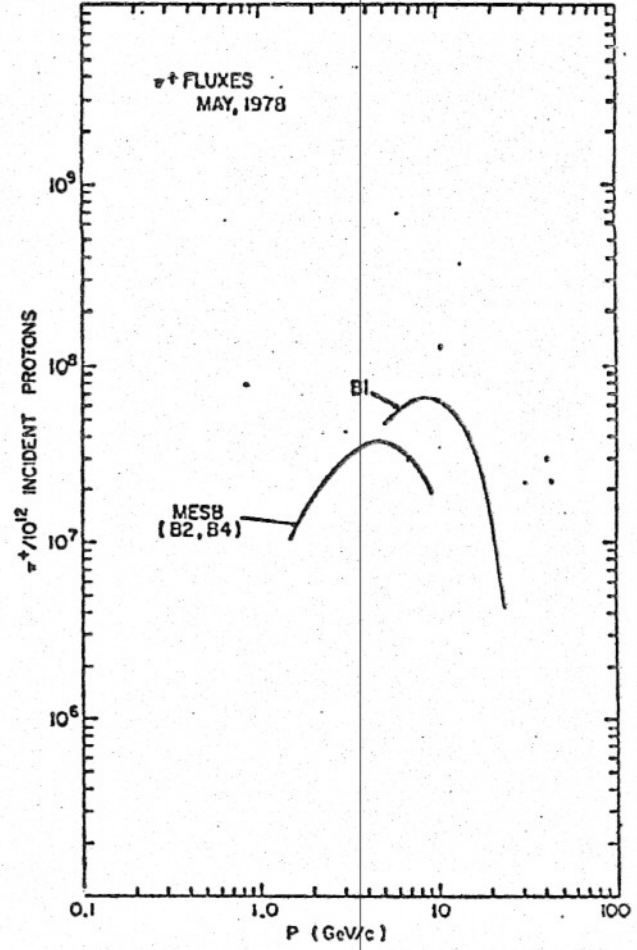
1. DTF Layout.
2. Fluxes Available in the MESB and B1.



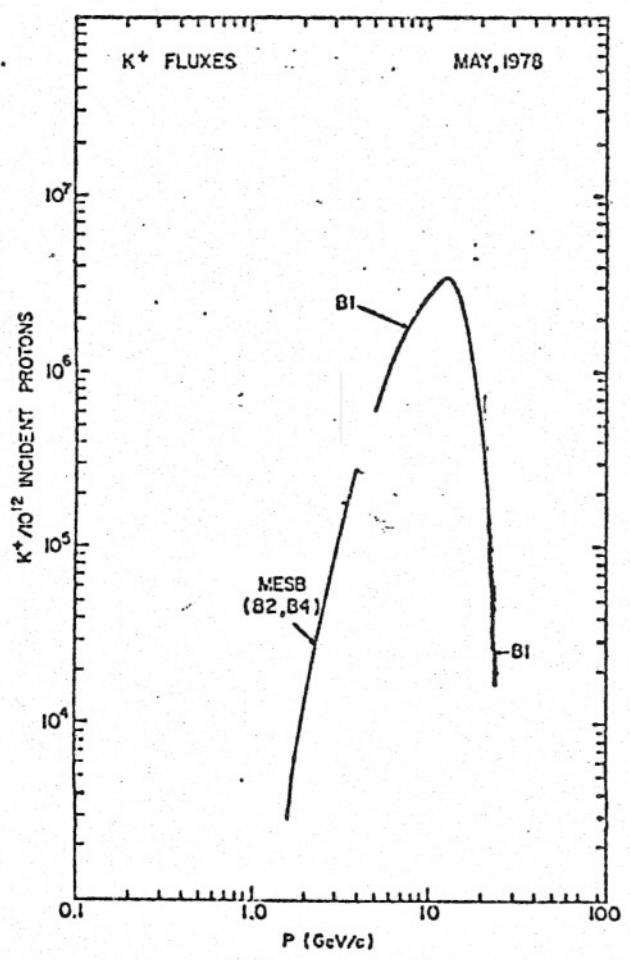
E14400 E14600 E14800 E15000 E15200 E15400 E15600 E15800
 N4500 N4600 N4700 N4800 N4900 N5000 N5100 N5200
 455 456 457 458 459 460 461 462 463 464 465 466 467 468 469 470 471 472 473 474 475 476 477 478 479 480 481 482 483 484 485 486 487 488 489 490 491 492 493 494 495 496 497 498 499 500
 2441 2442 2443 2444 2445 2446 2447 2448 2449 2450 2451 2452 2453 2454 2455 2456 2457 2458 2459 2460 2461 2462 2463 2464 2465 2466 2467 2468 2469 2470 2471 2472 2473 2474 2475 2476 2477 2478 2479 2480 2481 2482 2483 2484 2485 2486 2487 2488 2489 2490 2491 2492 2493 2494 2495 2496 2497 2498 2499 2500



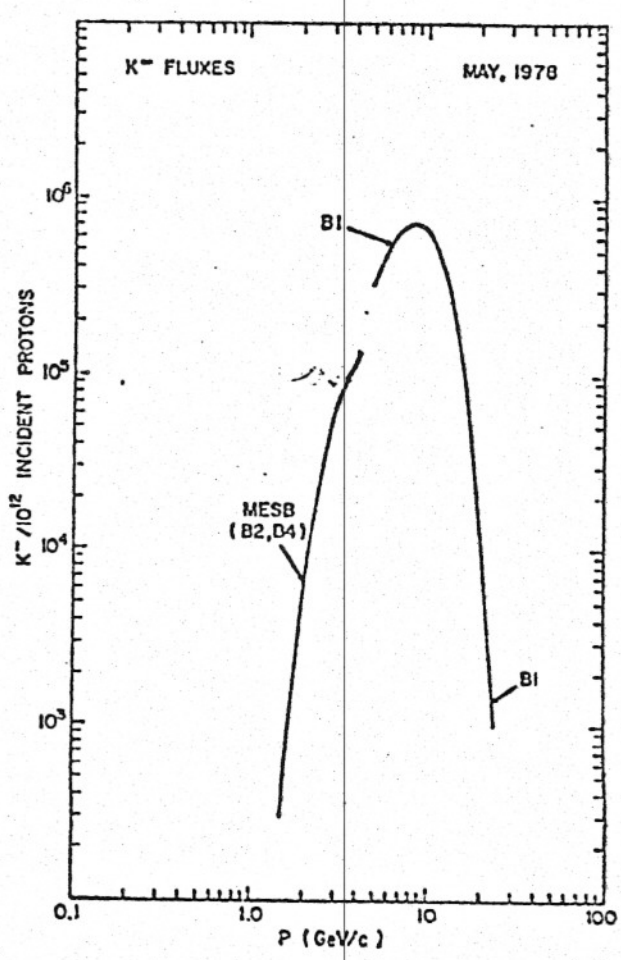
(a)



(b)

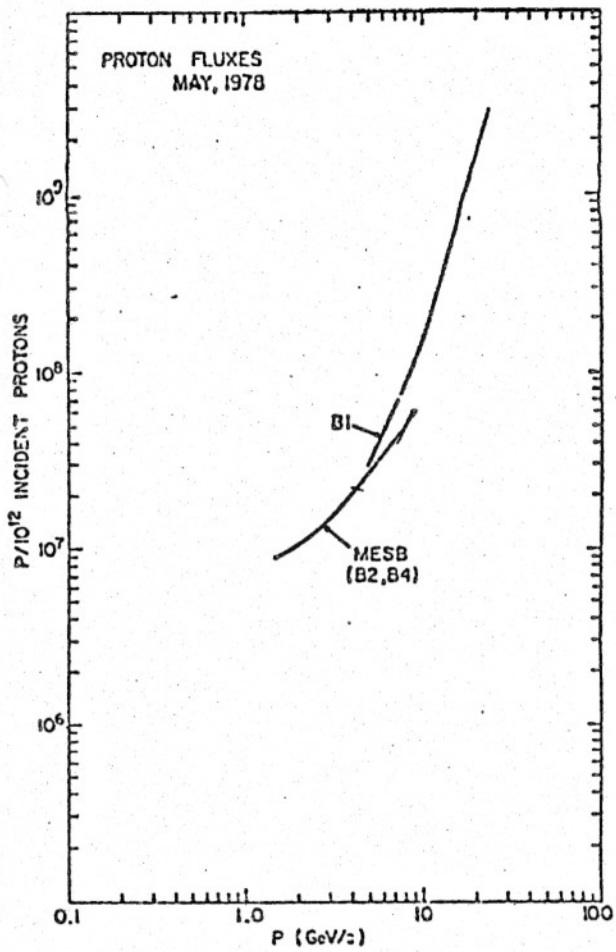


(c)

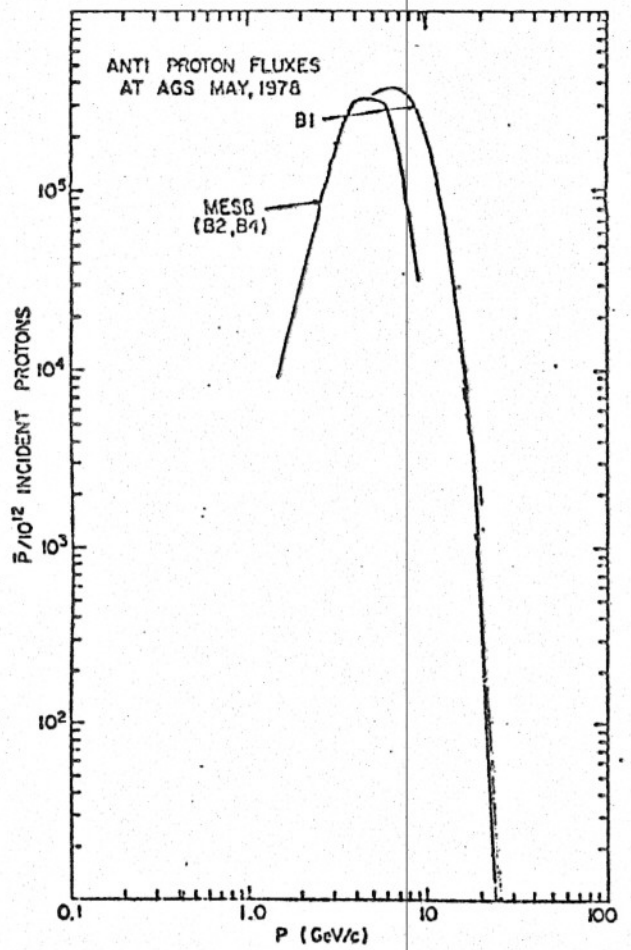


(d)

Fig. 2 (a-d)



(e)



(f)

Fig. 2 (e-f)

BROOKHAVEN NATIONAL LABORATORY
Associated Universities, Inc.
Upton, New York

ACCELERATOR DEPARTMENT
Informal Report

CHARACTERISTICS OF MESB: DESCRIPTION FOR USERS

C.T. Murphy* and J.D. Fox⁺
January 28, 1974

- * Present Address: National Accelerator Laboratory, Batavia, Illinois
+ Present Address: Saclay, Centre d'Etude Nucleaire de Saclay, France

ABSTRACT

The beam optical design and calculated performance data are presented for the Medium Energy Separated Beam from the "B" target station. Various modes of operation which enable the beam to separate kaons to 6 GeV/c, and anti-protons to 9 GeV/c are discussed. Purified particle fluxes in excess of 10^5 K^+ , 5×10^4 K^- , and 10^5 p per 10^{12} protons interacting in a beryllium target are anticipated.

NOTICE

This report was prepared as an account of work sponsored by the United States Government. Neither the United States nor the United States Atomic Energy Commission, nor any of their employees, nor any of their contractors, subcontractors, or their employees, makes any warranty, express or implied, or assumes any legal liability or responsibility for the accuracy, completeness or usefulness of any information, apparatus, product or process disclosed, or represents that its use would not infringe privately owned rights.

Introduction

The Medium Energy Separated Beam (MESB) is a one-stage, DC separated beam from the AGS external proton beam target B, designed to purify K's up to 6.0 GeV/c and \bar{p} 's up to 9.3 GeV/c for electronic experiments. The momentum limit is determined by the measured $fBdl$ of the first bending magnet at full current.

MESB was originally designed by Carroll¹ to separate 5 GeV/c K's and 8 GeV/c \bar{p} 's. Fox² increased the upstream bend angle in order that the beam reach the MPS (multiparticle spectrometer), added a quadrupole to the front-end doublet so as to approximately double the low momentum flux, and arranged a Y branch in the downstream end. This third effort on the beam design has resulted in a full utilization of the variable-focal length properties of the front-end triplet so as to increase the momentum-limit of separability.

Some details remain to be studied -- most notably, the optimum target material and length, multiple scattering in the Cerenkov counters, beam instrumentation and how to tune the beam, and muon contamination. Hence both the flux and the remaining contamination are somewhat uncertain: only lower limits can be set on both. What is firm is the position and number of elements in the beam, which have been determined by the sometimes conflicting requirements of momentum recombination and adequate K- π separation in both branches and the several modes of the beam. In addition, the placement of the final two quadrupoles in each branch of the beam is regarded as experiment-dependent and has been studied only for 5 approved experiments. It is the responsibility of each experimental group to decide on the placement of the last two quadrupoles and the position of the first horizontal focus.

The purpose of this note is to familiarize potential users with the certain aspects of the beam and invite participation and assistance in the resolution of the uncertain details of the tail end of the beam. First, the beam optics are discussed in a cursory fashion; then probable fluxes, purity, and spot sizes (or phase spaces) at the final focus of the beam are discussed.*

Layout

The layout of the beam is shown in Fig. 1. At the upstream end, the beam accepts particles at a 6° production angle from a target shared simultaneously with the 0° unseparated beam. At the downstream end, the beam serves experiments non-simultaneously at two places: (a) the East branch, in the region between MPS and the 0° experiments; (b) the West branch, or MPS. These branches are hereafter abbreviated E and MPS (or W).

Variable Focal Length Front Triplet: Modes 1-3

The variable-focal length triplet, Q1-2-3, allows the $K-\pi$ separation at the first vertical focus (the mass slit) to be held constant at twice the magnified, unaberrated, target height (a condition referred to hereafter as " $\eta = 2$ ") as the momentum is increased, in a continuous manner. As the momentum increases, the vertical focal length (f_v) increases and

* More detailed documentation on the beam exists in the form of EP&S Technical Notes: MESB Design Notes, referred to here just as Design Note:

- I. Tolerances on the Uniformity of f_{Bd1} in D1 and D2 (EP&S No. 59).
- II. Mass Slit Operation and Pion Contamination (EP&S No. 62).
- III. The Midsection: Variable Position of Horizontal Focus, Two Sextupoles, and Vertical Chromatic Aberration.
- IV. Annotated BEAM Output and Input.

the vertical acceptance angle (y'_t) decreases, in proportion. However, there are upper and lower limits in this variation. The lower limit, designated as mode 1 of the beam, occurs when Q3 is horizontally filled to its maximum usable aperture of about 5.5". The optics of this mode are illustrated in Fig. 2, for the first half of the beam. In this mode, $f_v = 270''$, $y'_t = 3.7$ mrad, and the beam separates with $\eta \geq 2$ up to 4 GeV/c K's and 6.3 GeV/c \bar{p} 's. This mode is a lower limit because lowering the vertical focal length any further leads to greater losses in horizontal acceptance angle than gains in vertical acceptance angle. Hence experiments below 4 GeV/c can do no better than to run in mode 1. The upper limit, designated as mode 3, has the polarities of Q2 and Q3 reversed from those of mode 1 and is defined as the point at which the vertical focal length is a maximum (850"). The optics are shown in Fig. 3. This mode separates 6 GeV/c K's and 9.4 GeV/c \bar{p} 's with $\eta = 2$. The gradients in the triplet are shown as a function of momentum (as the focal length is gradually increased to 850") in Fig. 7.*

Table I lists the properties of the beam up to the mass slit for modes 1, 3 and 4 (mode 4 is explained later) in the East and West branches. Gradients and bending magnet fields are listed in Table II for 5 GeV/c only. For exact information on modes in between 1 and 3, a beam program such as BEAM must be run. Alternately, the following crude scaling can be applied: the solid angle decreases proportional to P^{-3} ; bending magnet fields and quadrupole gradients (excepting Q1-2-3) increase linearly with P, except

* Mode 2 is the point where the gradient of Q3 is zero. The mountain in the current required by Q1 as one moves continuously from mode 1 to mode 3 has been named after the physicist who first objected to the excessive power requirement of that mode. It is probable that the power supply initially assigned to Q1 will not permit running near mode 2.

for Q6, which is both mode and branch dependent. In the East branch the Q6 gradient increases as P^2 ; in the West branch, the gradient remains roughly constant.

Dispersion and Separation

The bending magnet D1 disperses the beam in the horizontal plane. Following Q3, four rectangular separators, assumed to operate at 225 kV/inch, separate K's from π 's in the vertical plane. The physical separation is achieved in the mass slit at the first vertical focus. A sextupole placed near the first horizontal focus (just after Q4) corrects most of the chromatic aberration in the vertical plane at the mass slit. The momentum bite of the beam is defined by a remotely variable collimator just downstream of the first sextupole.

As can be seen in Figs. 2 and 3, mode 3 will barely transmit a momentum bite of $\pm 2.5\%$ through Q4, while mode 1 could transmit $\pm 5\%$. However, K- π separation is aberration-limited with a bite of $\pm 3\%$ in mode 1, at least at 4 GeV/c where $\eta = 2$. At lower momenta, it might be possible to separate a bigger momentum bite.

Midsection

The midsection of the beam (Q4, Q5, D2, Q6, D3, D4) focuses vertically at the mass slit, recombines momenta in both angle and position and achieves the desired beam size at the entrance to the final doublet (experiment dependent). The optics differ immensely in the two branches and change from mode to mode. The following sketch is amplified in Design Note III.

D2 steers the beam towards D4 which switches the beam either to the MPS or to the open area between MPS and the 0° beam experiments. D2 and D4 alone would not quite get a 9.3 GeV/c beam to MPS, so D3 was added and put directly behind the mass slit in order to also sweep out low-energy particles produced in the mass slit. A sufficient drift space was necessary between D3 and D4 to allow D4 to be part of a beam spectrometer for momentum determination.

To first order, each of the three quadrupoles has a single function. Q4 is a field lens for off-momentum particles and steers them into D2-3-4 such that they emerge with the same angles as on-momentum particles. Q5 focuses vertically on the mass slit. Q6 centers off-momentum particles in D4 such that they emerge position-recombined. In the West leg, this requirement results in Q6 forming a nearly parallel beam (for on-momentum particles); in the East leg, the "unnatural" direction of the D4 bend requires that Q6 make an extra horizontal focus somewhat in front of D4. Therefore Q6 requires much more gradient in the East leg modes than in the West leg. Because of very strong second-order mixing of the functions of the quadrupoles, the gradients in Q4 and Q5 are also much larger in the East branch than in the West.

Control over the size of the beam at the entrance to the final doublet (or triplet) which focuses the beam on the experimental target is provided by allowing the position of the first horizontal focus to be variable. This flexibility is necessary in order to obtain downstream optics which are independent of mode (momentum). In most modes it was found that if the position of the first horizontal focus was the sextupole immediately following Q5, then the beam, tuned to be momentum recombined in both

position and angle, would enter the final doublet with a size roughly filling the first quadrupole of the doublet. However, in mode 1W, momentum recombination demanded that the next horizontal focus occur at the entrance of the final doublet, leading to a beam size at the experimental target which was very large. By moving the first horizontal focus 65" downstream, the downstream horizontal optics became roughly the same as in Mode 3W.

The general rule of thumb is the following: to make the beam bigger (horizontally) at the final doublet, move the first horizontal focus downstream.*

Moving the horizontal focus further downstream than the second sextupole (1753" from B target) brings about rapidly increasing beam losses on the 12" aperture of Q4, and is thus not recommended.

Correction of vertical chromatic aberrations with sextupoles still works even if the horizontal focus is not exactly at a sextupole. In the region between Q5 and D2, the beam is going out of focus so slowly that one can do just as good a job with the nearest sextupole as one would do with a sextupole exactly at the focus. If the focus is moved upstream of Q5 (as in East modes), it is advisable to get an extra power supply and power both sextupoles, one negative and one positive, in a ratio given in Design Note III. Numerical data supporting this paragraph also appear in that Note. The position of the first horizontal focus is a variable which the user can control and change.

* In Mode E1, there is a problem with scraping in Q6. It was found that this was relieved somewhat by moving the first horizontal focus upstream to the end of Q4. (Mode E3 has a scraping problem in the final doublet, which could probably be relieved by moving the first focus up to the end of Q4.)

Purity of Separation and Aberrations

The condition $\eta = 2$ which we have selected as a minimum condition of separability means that the center of the pions is separated from the center of the kaons at the mass slit by a distance of twice the geometrical image height, i.e., target height times magnification. If there were no aberrations, one could separate with $\eta = 1$. However, chromatic aberrations alone more than double the image widths, so that the K and π images are very overlapped in some modes.

The sextupole at the first horizontal focus would remove the chromatic aberration entirely if the width of the horizontal image (for a given momentum) were zero. However, the target appears to be very wide, specifically, the length (4") times $\sin 6^\circ$, which is 0.42", so that at the first horizontal focus the image of on-momentum particles touches the edge of the image of particles with $\Delta P/P = 2.5\%$. The result is that the sextupole removes only about half of the chromatic aberration. The K's and π 's remain overlapped.

A mass slit has been designed which intercepts π 's in the overlapped region of phase space (at the expense of intercepting up to 22% of the K's), and is fully documented in Design Note II. In summary, that Note shows that with the criterion of $\eta = 2$ (which defines the highest momentum at which modes 1 and 3 can be used) the π/K ratio at the experiment is predicted to be between 0.26 (Mode 1E) and 1.80 (Mode 3E). These are lower limits because no other aberrations have been quantitatively studied (except the sextupole component of D1 -- see Design Note I and Figs. 12 and 13 of this document).

Other potential aberrations are separator non-uniformity or instability, quadrupole aberrations, and scattering from magnets and the momentum

collimator in the region between the separators and the mass slit. Undocumented hand calculations indicated that separator and quadrupole aberrations were insignificant. The scattering problem has been given no thought.

Purity can always be improved, of course, by running in a mode in which $\eta > 2$, e.g., using Mode 3 for 5 GeV K^- .

Moving Q6 for Mode 3E

It was found that most of the chromatic aberration in Mode 3 (East or West) came from the Q4-5-6 triplet. In Mode 3E (and only Mode 3E) it was found that a significant reduction in the π/K ratio was achieved by moving Q6 downstream by 150" from its normal position (moving it further downstream pushed the gradient too high). The reduction in the π/K ratio, was roughly a factor of 2. Data quoted for Mode 3E assume this change. However, it seems prudent to verify experimentally this improvement before accepting such a rerigging problem as part of the demands of experiments in the East leg.

Mode 4

Chromatic aberration is reduced by a factor of 2 at the mass slit by reversing the polarity of Q4-5, as explained in Design Note III. However, off momentum particles with $\Delta p/p \geq 1.5\%$ are then lost in Q4, so the total flux is reduced. This mode is as pure in π/K ratio at 6.6 GeV as Mode 3 is at 6 GeV/c, in our computer idealization, so that this mode might extend the usable momentum range of the beam for kaons up to 6.6 GeV/c. Alternately, this mode is a safety valve for approved experiments at 6 GeV, should the K/π ratio prove to be intolerable in Mode 3.

Downstream Optics

The position of the final focusing elements is the responsibility of the user. However, a number of arrangements for approved experiments have been studied and are presented as examples. The properties of the beam at the final focus for these examples are shown in Table III.

The spot sizes shown in Table III include chromatic aberration only, and do not include the important effect of multiple scattering in the beam Cerenkov counters, an effect which is both momentum and experiment dependent (see below).

In the East leg D. O'Brien selected the positions for D4, Q7 and Q8 and decided to leave D3 off in order not to place the experimental area too close to the 0° beam experiments.*

The final focus in Mode 3 of the West leg has been studied for three arrangements of the final focusing elements. The first, called 3WCAM tries to cram the beam into a small 12" target. The width, ΔX , is small and the divergence ($\Delta X'$) is large. The spacing of Q7-8 is quite large. Mode 1W has been studied only for the CAM conditions (Column 1, Table III).

The mode called 3WCMU is the arrangement created for the CMU experiment, which wanted a spot which would fit inside a 3" LH2 target in front of the MPS magnet but would be reasonably small in a beam anti-counter 385" downstream of the LH2 target. The vertical focus is actually 240" downstream of the LH2 target. The size of the beam at the anti-counter (100% of particles, but no multiple scattering) is 6" x 1.7".

* Extensive studies of this leg were written by O'Brien. We disagree with his estimates of $K:\pi$ ratio (see Design Note II) and find no mention of the serious (25%) scraping problem in Mode 3E (see Table III, last row). This scraping problem might be cured by moving the first horizontal focus upstream of its current position (1623") or by moving Q7-8 upstream.

The mode called 3WROT uses a triplet, rotated 45° from the normal orientation, to perform an imperfect interchange (or rotation) of the x and y phase spaces. The details are the subject of a separate note (Design Note IV). This rotation is desirable for experiments which need a small horizontal phase space.

In principle, the horizontal phase space ($\Delta X \Delta X'$) and vertical phase space ($\Delta y \Delta y'$) should be the same in all modes (Liouville's theorem). Excepting mode 3WCRAM, the theorem holds within 20% for the horizontal plane but only within a factor of 4 for the vertical plane. The variations result from differing amounts of chromatic aberration in the various modes. The phase spaces in Mode 4 are smaller since the momentum bite is only $\pm 1.5\%$; the horizontal phase spaces in the East leg are bigger because of the increased focusing necessary in order to have three horizontal foci.

Perfect interchange of phase space in Mode 3WROT would result in a vertical phase space of ~ 24 mr-inches and a horizontal phase space of ~ 1 mr-inch. In fact the two numbers turn out to be 29 mr-inches and 4.4 mr-inches. The factor of 4 increase in the horizontal phase space comes half from the increased chromatic aberration of the triplet and half from the fact that it takes at least four quadrupoles to do an exact rotation.

Fitting four quadrupoles into the line, with spacings adequate to keep gradients low enough, was proven impossible. In order to perform the imperfect interchange documented here, using the two 12Q30's assigned to MESB plus a borrowed 8Q48, the spacings had to be lengthened such that the beam momentum spectrometer arm following D4 is shortened by a couple of feet in order to keep gradients low enough that 9.3 GeV/c is achievable.

Multiple Scattering in the Beam Cerenkov Counters

Three threshold beam Cerenkov chambers are being built by CMU, two of which distinguish π 's from K's, one of which distinguishes K's from p's (or \bar{p} 's). The gas will be ethane.

Edelstein⁴ has calculated that the K-p counter, operating at 270 psi at 3 GeV/c, will cause 2 mr (not projected) of multiple scattering (rms). This number is large compared to the natural divergence of the vertical plane (2 mr) in most modes, and so could cause a very large broadening of the image. This problem has been discovered only recently and has not been studied carefully. The remainder of this section gives sufficient information so that the user can calculate the effect for his experiment, and select Cerenkov positions which minimize the effect.

The multiple scattering is very momentum dependent. In the simple assumption that the counter is actually operating at threshold, the mean multiple scattering angle is proportional to m/p^2 , where m is the mass of the particle and p is the momentum. The windows on the counter are the dominant source of scattering at high momenta. At 3 GeV, using kaons, there are 2 mr multiple scattering in the gas and 1.1 mr in the window. At 6 GeV/c there is 0.6 mrad multiple scattering in both the gas and the windows.

To translate mean multiple scattering angles into mean broadening at the final focus is trivial for a Cerenkov counter in the drift space preceding the final focus. For counters upstream of the last quadrupole the calculation requires a well-known theorem from beam optics. If a scattering, $\delta\theta_p$, occurs in the vertical plane at some point P along the beam, then the deviation in y of the ray traced back to the target, δy_t , is given by

$$\delta y_t = b_p \delta\theta_p$$

where b_p is the (1,2) matrix element in the transfer matrix relating rays at the target to rays at p:

$$\begin{pmatrix} y_p \\ y'_p \end{pmatrix} = \begin{pmatrix} a_p & b_p \\ L_p & d_p \end{pmatrix} \begin{pmatrix} y_t \\ y'_t \end{pmatrix}$$

The value of b_p at any point along the beam can be calculated for any mode from the paraxial ($y_t = 0$) ray traces of Figs. 2-6:

$$b_p = \frac{y_p}{y'_t}$$

where $y'_t = 0.00368$ rad for mode 1 and 0.00115 rad for mode 3. The deviation at the final focus is simply δy_t times the vertical magnification given in Table III:

$$\delta y_f = m_v \frac{y_p}{y'_t} \delta \theta_p \quad (2)$$

For example, suppose there is an rms multiple scattering of ± 1 mr in the vertical plane in a Cerenkov counter placed just behind Q7 in mode 3WCRAM, where $y_p \approx 1''$. Then

$$\delta y_f = \pm \frac{(0.75)(1)(.001)}{(.00115)} = \pm 0.65''$$

This is large compared to the predicted final spot size of 0.2''.

The same theorem applies to the horizontal plane but leads to less disastrous broadening because $x'_t = 20$ mr. To minimize multiple scattering the K-p Cerenkov counter should be placed at a place where y_p (or x_p) is small, i.e., near a focus. Some users may wish to put one of the Cerenkov counters behind D3, at the cost of shortening the beam spectrometer.

It is not clear how to do the calculation for mode 3WROT in which the vertical and horizontal planes are mixed.*

Intermediate Modes and Program BEAM

Up-to-date output for modes between 1 and 3 do not exist. During the design, mode 2 was occasionally run and seemed to have no problems.

The simplest way to obtain output for intermediate modes is to use the program BEAM because self-tuning input decks already exist. The program and input decks can be obtained from the EP&S group. One simply changes the value of Q1, using Fig. 7; input cards in the deck then tune all other quadrupoles, demanding foci in the correct places and momentum recombination in angle and momentum. If the change in the value of Q1 is large, the focusing routines may not converge; in that case several runs need to be made, moving Q1 in steps towards the desired value and inserting the latest set of quadrupole gradients for each run.

Program BEAM has the disadvantage that there is no documentation other than Design Note V. Comment cards are fairly generous however.

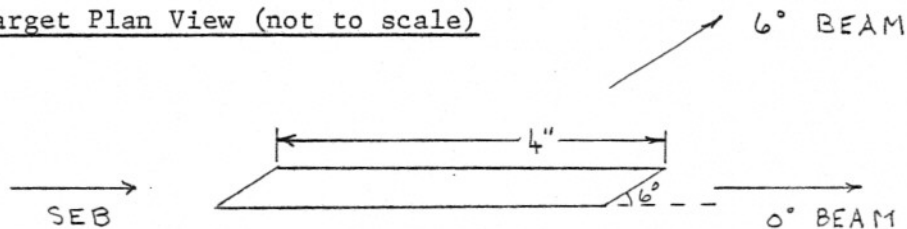
Target Design

The properties of the beam listed in Table I assumed a target of dimensions (height, width, length) = (0.04", 0.10", 4"). It is hoped that it can be shaped as shown below.

* Program BEAM has an input card reserved for multiple scattering elements; however, this branch of the program is now inoperative. Comment cards in subroutine TRACE indicate how to reinstitute the branch.

Conservative estimates of fluxes have been made using the data on production in beryllium of Sanford and Wang.³ Extrapolations to heavier nuclei are uncertain because of reabsorption in the struck nucleus. It is estimated that for K^- perhaps a gain of a factor 2 (per inch of target length) can be achieved using copper instead. The optimization problem has yet to be studied in detail, and is probably experiment dependent. In addition, the target must satisfy the requirements of the 0° beam.

Target Plan View (not to scale)



At the moment, 5 targets have been designated to be available on the target table: 4" Be, 2" Be, 4" Cu, 2" Cu, and 2" W. All will be shaped as shown above.

Fluxes

Fluxes can be calculated with the aid of Figs. 8-10, which give yields at the final foci per 10^{12} interacting protons in beryllium at 6° (phase I) and 3° (phase II). The dotted curves show the yields in modes 1 and 3 assuming the full solid angles and momentum bites of Table I; the solid curves show the yield as one gradually varies the focal length of the front triplet, moving continuously from mode 1 to

mode 3. For K^{\pm} above 6 GeV, mode 4 is shown. Otherwise, the curves include the effect of 70% transmission of the full solid angle and momentum bite through MESB, a figure resulting from Monte Carlo studies.

To obtain the true flux in the beam, one must fold in the number of protons in the external beam and the fraction which interact in the target. If 4" of beryllium is used, this fraction might be 1/6, assuming that all protons hit the target. It is hoped that this estimate is conservative.

Approximately the same results were obtained by O'Brien using Hagedorn-Ranft particle production curves.

Momentum Bite

The momentum bite in the MESB will not be very sharply defined because of the very large effective target width. At the momentum collimator, the image of on-momentum particles touches the edge of the image of particles with $\Delta P/P = 2.5\%$. Fig. 14 shows the momentum spectra expected in modes 1 and 3 when the momentum collimator is set at the center of the image of particles with $\Delta P/P = \pm 3.0$ and 2.5%, respectively. The rule-of-thumb is that the momentum distribution always extends 1% beyond the desired bite.

The momentum bite is slightly more sharply defined for mode 1W than for 1E, as a result of the fact that the horizontal focus for mode 1E is not at the collimator but upstream of Q5.

Momentum Determination

In the West leg, a beam spectrometer of proportional wire chambers around D4 will determine the momentum of individual particles to $\pm 0.25\%$. An independent spectrometer is planned for the East leg.

Beam Size at Various Magnets

For guidance in designing detection devices, Table IV gives the spot size of the beam (100% of the particles) at various points along the beam.

Collimators

A remotely variable horizontal collimator follows Q1. A fixed aperture (2") collimator is planned to be inserted in Q3. To degrade muons and stop secondaries from the mass slit, D3 has a vertical aperture of 1.25 inches. A remotely variable horizontal collimator just after the first sextupole determines the momentum bite. Both remotely variable horizontal collimators have separate drives for the right and left plate. Both are made of heavimet.

In mode 3E the mass slit is also a horizontal focus, so the mass slit should be followed by a horizontal stop which can be crude, as it will be in air. The corresponding horizontal focus in mode 1E is just in front of D4, where it would be desirable to have the possibility of a horizontal collimator. However, none is planned.

The square pipe through the steel proton beam shield wall in the middle of the separators is a natural vertical collimator. It would be wise to put a fixed aperture horizontal collimator inside Q4 in order to remove very off-momentum particles from the bad-field region of Q4. These

off-momentum particles will not necessarily be removed by the momentum collimator.

Phase II

The layout as shown is called phase I. It is actually not very usable above 7 GeV for \bar{p} 's, as the flux at a 6° production angle is falling very fast (see Fig. 10). Hence a phase II of the MESB is envisaged in which a septum bending magnet is added in front of Q1 which will bend particles produced at 3° towards the fixed bend point of D3; Q1 and Q2 are moved inward a few inches. The rest of the beam remains intact and then will transport up to 9.3 GeV/c, limited entirely by D1. The \bar{p} flux should increase by a factor of 3 at 7 GeV/c and a factor 6 at 10 GeV/c. Phase II also has the fringe benefit of reducing two problems associated with the large apparent width of a 4" long target viewed at 6° . This large apparent width creates a rather large horizontal phase space, so that small spot sizes are difficult to achieve. Secondly, this large width induces large aberrations in the vertical plane in mode 3 at the mass slit, making separation very marginal. In phase I, the only cures available, such as halving the target length, result in a loss of flux. With a 4" target in phase II (3° production), both the vertical plane aberrations and the horizontal spot size are dominated by other effects (largely chromatic aberration).

Acknowledgements

Useful suggestions and criticisms have been received from D. Berley, H. Brown, A. Carroll, and H. Foelsche. The program used was written by J. Fox. E. Makuchowski provided much assistance in altering and executing the computer program. E. Willen edited the final draft and the figures.

B1, B2 Distribution

References

1. A. Carroll, Summer Study on AGS Utilization, 1970.
2. J.D. Fox, EP&S Division Technical Note No. 38, 1970.
3. J. Sanford and C.L. Wang, AGS Internal Report, 1967.
4. Note on Beam Cerenkov Counters for MESB/MPS, R.M. Edelstein, May 1973.

TABLE I - Properties of MESB Phase (Production) up to the Mass Slit

Definitions:

$$\eta_K \equiv \frac{K-\pi \text{ separation at mass slit}}{\text{magnified geometrical target height}}$$

$$\theta_V \equiv \text{vertical plane divergence}$$

$$\theta_H \equiv \text{horizontal plane divergence}$$

Front End	Mode 1	Mode 3	Mode 4
Max. θ_V	± 3.68 mr	± 1.15 mr	± 1.15 mr
Max. θ_H	± 20 mr	± 20 mr	± 20 mr
Ω (geometrical solid angle) = $4\theta_V\theta_H$	294 μsr	92 μsr	92 μsr
Assumed production target (height x width x length)	.04" x 0.10" x 4"	.04" x 0.10" x 4"	.04" x 0.10" x 4"
f_V (vertical front focal length)	274"	860"	860"
momentum at which $\eta_K = 2$	4.0 GeV/c	6.0 GeV/c	6.6 GeV/c ($\eta=1.5$) [‡]
momentum at which $\eta_p^- = 2$	6.3 GeV/c	9.4 GeV/c	9.4 GeV/c

At first horizontal focus	1W	3W CRAM	3W CMU	3W ROT	4W	1E	3E	4E
distance from target	1688"	1623"	1753"	1753"	1623"	1517"	1623"	1545"
$\pm \Delta P/P$ (max. momentum bite)	$\pm 3.0\%^*$	± 2.5	± 2.5	± 2.5	± 1.5	$\pm 3.0\%^*$	± 2.5	± 1.5
dispersion at momentum collimator [†]	0.89"/%	1.27"/%	1.20"/%	1.08"/%	2.46"/%	1.00"/%	1.78"/%	2.54"/%
horizontal magnification	3.2	6.3	5.7	5.5	13.0	3.6	4.8	12.6
horizontal image full width (on momentum)	1.34"	2.62"	2.24"	2.32"	5.52"	1.50"	2.0"	5.3"

At mass slit	1W	3W CRAM	3W CMU	3W ROT	4W	1E	3E	4E
distance from target	2152"	2152"	2152"	2152"	2152"	2152"	2152"	2152"
vertical magnification	2.41	0.63	0.65	0.59	1.00	2.3	0.58	1.40
K- π separation at momentum where $\eta = 2$	0.194"	0.050"	0.054"	0.047"	0.060" [‡]	0.184"	0.046"	0.084" [‡]
max. θ_V	$\pm 1.52\text{mr}$	$\pm 1.83\text{mr}$	$\pm 1.77\text{mr}$	$\pm 1.95\text{mr}$	$\pm 1.15\text{mr}$	$\pm 1.60\text{mr}$	$\pm 2.00\text{mr}$	$\pm 0.82\text{mr}$
horizontal full width	6.0"	6.0"	5.4"	5.4"	4.2"	5.4"	5.4"	4.0"

*Could transmit $\pm 5\%$, badly aberrated

†The momentum collimator is at 1663" from the B target, which is never exactly at the focus.

‡Mode 4 is as pure at $\eta = 1.5$ as mode 3 is at $\eta = 2$ because of reduced chromatic aberration.

TABLE II

Gradients and Fields in MESB at 5 GeV/c

In scaling to other momenta, only the bending magnets behave linearly. To scale Q1-Q2-Q3, see Fig. 7. To scale Q4-Q5-Q6, see text. Q7-Q8 scale roughly linearly. For exact information, a computer run is necessary. All bend angles are 8° except D3, which is 3.07° in the West branch and 0° in the East. Positive gradients are focussing horizontally.

Magnet	Type	Vert. Gap or Diam.	Eff. Length	Position (B-targ. to center)	Fields (kG) or Gradients (kG/inch)								Max Field
					1W	3W CRAM	3W CMU	3W ROT	4W	1E	3E	4E	
Q1	N8Q32	8"	36"	180"	1.55	0.95	0.95	0.95	0.95	1.55	1.55	0.95	3.3
Q2	N8Q32	8	36	277	- 1.59	+ 0.57	0.54	0.54	0.58	- 1.62	0.57	0.58	3.3
D1	18C72	3.5	75.5	360	12.10	12.10	12.10	12.10	12.10	12.10	12.10	12.10	22.5
Q3	12Q30	12	36	433	0.69	- 0.65	- 0.65	- 0.65	- 0.65	0.75	- 0.65	- 0.65	2.7
Q4	12Q30	12	36	1499	0.84	0.97	1.01	1.07	- 0.89	1.42	1.20	- 1.03	2.7
Q5	8Q24	8	28	1579	- 1.31	- 1.40	- 1.43	- 1.45	+ 1.37	- 1.70	- 1.48	1.79	3.6
S1	12S24	12	26.5	1608	- 0.60*	- 0.12*	0	0	- 0.18*	*	- 0.16*	?	1.25
S2	12S24	12	26.5	1721	0	0	- 0.28*	- 0.34*	0	*	0	?	1.25
D2	18D72	2.5	74	1870	12.34	12.34	12.34	12.34	12.34	12.34	12.34	12.34	25
Q6	8Q24	8	28	1943 [†]	0.91	0.67	0.75	0.58	- 0.06	1.18	1.69	1.82	3.6
D3	18D36	1.25	42	2202	8.34	8.34	8.34	8.34	8.34	0	0	0	20.5
D4	18D72	2.5	74	2446(W) 2472(E)	12.34	12.34	12.34	12.34	12.34	12.34	12.34	12.34	25
Q7	12Q30	12	36		- 0.99	- 1.00	+ 1.45	1.21	- 1.29	- 1.61	- 1.57	- 1.56	2.7
Q8	12Q30	12	36		1.44	1.48	- 1.52	- 1.45	1.51	2.26	2.24	2.23	2.7
Q9	8Q48	8	52		-----	-----	-----	1.55	-----	-----	-----	-----	2.5 or 3.6

* The x component of the field of a sextupole is given by $B_x = Ksy$. The "Gradient" listed is $fKd\theta$.

[†] 2093" in mode 3E.

TABLE III. Properties of the MESB at Various Final Foci

The full widths (Δx , Δy) include 95% of the particles, but do not include the large effects of multiple scattering in the beam Cerenkov chambers. The full angles ($\Delta x'$, $\Delta y'$) include 99% of the particles. The transmission is the fraction of the particles in the initial phase space (see TABLE I) which reach the second focus; the average transmission (70%) has been folded into the flux curves (Figs. 8-12). See text for discussion.

	MODE							
	1W	3W CRAM	3W CMU	3W ROT	4W	1E	3E	4E
Distance from B-targ. to:								
Q7 Center	2796"	2796	2796	2645	2796	2645	2645	2645
Q8 Center	2984"	2984	2874	2845	2904	2753	2753	2753
Q9 Center	---	---	---	3015	---	---	---	---
Target Magnification at final focus:								
MV	3.51	0.75	0.25	0.53	1.05	2.66	0.60	1.33
MH	1.20	1.79	4.33	0.53	1.77	0.57	0.53	1.17
Full widths at final focus:								
Δx	0.45"	0.38	1.6	0.40	0.40	0.45	0.40	0.40
$\Delta x'$	52 mr	60	15	11	44	64	80	52
Δy	0.25"	0.19	0.20	1.3	0.10	0.20	0.20	0.20
$\Delta y'$	4.4 mr	4.0	9.0	22	2.4	5.6	5.6	3.2
$\Delta x \Delta x'$	23 mr"	23	24	4.4	17	29	32	21
$\Delta y \Delta y'$	1.10 mr"	0.76	1.8	29	0.24	1.1	1.1	0.64
Transmission	77%	72	75	70	74	65	61	77
% which scrape Q8	3%	3	0	5	7	0	20	0

TABLE IV. Approximate Beam Sizes at Various Places Along the Beam

The quantity listed is $(\Delta x) \times (\Delta y)$, where Δx = horizontal full width, Δy = vertical full width, in inches. These widths include 100% of the particles (or more, in the case of Δy where the histogram bin size is sometimes too big). The widths are based on ray plots up to PLIM and on Monte Carlo's thereafter. In the MPS modes, sizes beyond the mass slit depend upon the final focussing method as shown. "CRAM" is the small horizontal spot size with large divergence. "CMU" is the big horizontal spot size with small divergence. "ROT" is phase space interchange with a rotated triplet. Full momentum bite and a 4" B-target are assumed. MPS1 is blank frequently since it has not been studied past MASS.

MODE Position	E1	E3	MPS1			MPS3			MPS4
			CRAM	CMU	ROT	CRAM	CMU	ROT	CRAM
Q3 end	10.6x2.0	6.0x2.0	11.0	x	2.0	4.8	x	2.0	4.8x2.0
Q4 end	12.0x3.2	12.0x2.6	11.0	x	3.0	12.0	x	2.0	8.5x2.0
PLIM*	1.8x3.0	4.4x2.6	5.3x3.3			6.3x2.5	6.0x2.5	5.5x2.5	7.4x1.1
Q6 end	8.4x0.8	6.0x0.4	8.4x0.8			8.4x0.8	7.8x0.8	6.0x1.2	4.8x0.8
Mass Slit [†]	5.4x1.3	5.4x0.3	6.0x1.3			6.0x0.3	5.4x0.3	5.4x0.3	4.2x
D3 end	4.2x0.8	3.6x0.6	6.0x0.4			5.4x0.4	4.2x0.4	5.4x0.4	4.2x0.4
D4 end	3.6x1.6	5.4x1.8	5.4x1.6			5.4x1.6	6.0x1.6	7.2x1.2	6.0x1.2
Q7 begin	5.6x2.0	8.8x2.4	8.0x2.4			8.0x2.6	10.4x2.6	8.0x1.6	9.6x1.6
Q8 begin	10.4x1.0	18.0x1.2 [‡]	16.0x1.2 [‡]			16.0x1.2 [‡]	6.4x4.2	11.2x11.2	16.0x1.0 [‡]
Q8 + 44"	6.5x0.4	8.4x0.8	9.0x0.8		---	9.0x0.8	4.5x4.0	-----	10.8x0.8
Q9 begin	-----	-----	-----	---		-----	-----	2.5x6.0	-----
Q9 + 44"	-----	-----	-----	---		-----	-----	2.0x4.0	-----
MPS-targ.	-----	-----	0.6x0.5			0.5x0.2	2.2x2.6 ⁺	0.4x1.1	0.5x0.2
East-targ.	.60x.65	0.75x0.35	-----	---	---	-----	-----	-----	-----

* Momentum collimator, assumed to be set at the center of image of off-momentum particles at full bite.

† In vertical plane, includes π^+ 's, K^+ 's and \bar{p}^+ 's, at momentum where $\eta = 2$.

‡ Scrapes.

+ LH2 target in front of MPS magnet.

Figure Captions

- Fig. 1 Beam Layout
- Fig. 2 Optics of Mode 1E
- Fig. 3 Optics of Mode 3E
- Fig. 4 Optics of Mode 1W
- Fig. 5 Optics of Mode 3W CRAM
- Fig. 6 Optics of Mode 4W
- Fig. 7 Gradients of quadrupoles Q1, Q2, Q3 vs. momentum at which $\eta = 2$, for K separation and \bar{p} separation.
- Figs. 8 - 10 Fluxes of particles at the two final foci per 10^{12} interacting protons in a beryllium target, assuming Sanford + Wang. The curves assume the full solid angle and momentum bites of Table I and a 70% transmission through the beam. For genuine numbers of particles at the end of beam, multiply by the number of protons in the external beam and the fractions which interact in the target.
- Fig. 11 $\pi^-:K^-$ and $\pi^-:\bar{p}$ ratio in front of mass slit as a function of momentum.
- Fig. 12 Variation of $\int B d\ell$ as a function of horizontal position in D1.
- Fig. 13 $\int B d\ell$ as a function of current for D1. The measured values extend to 3.0 kA. Taking $\int B d\ell / I = 500$ kG in /kA at 3.4 kA gives $P_{\max} = 9.24 \pm .2$ GeV/c. For 510 kG in /kA, $P_{\max} = 9.43$ GeV/c.
- Fig. 14 Expected momentum distributions for several modes. The momentum collimator was set at the centers of the images of particles with $\Delta p/p = \pm 3\%$ and $\pm 2-1/2\%$ for modes 1 and 3, respectively.

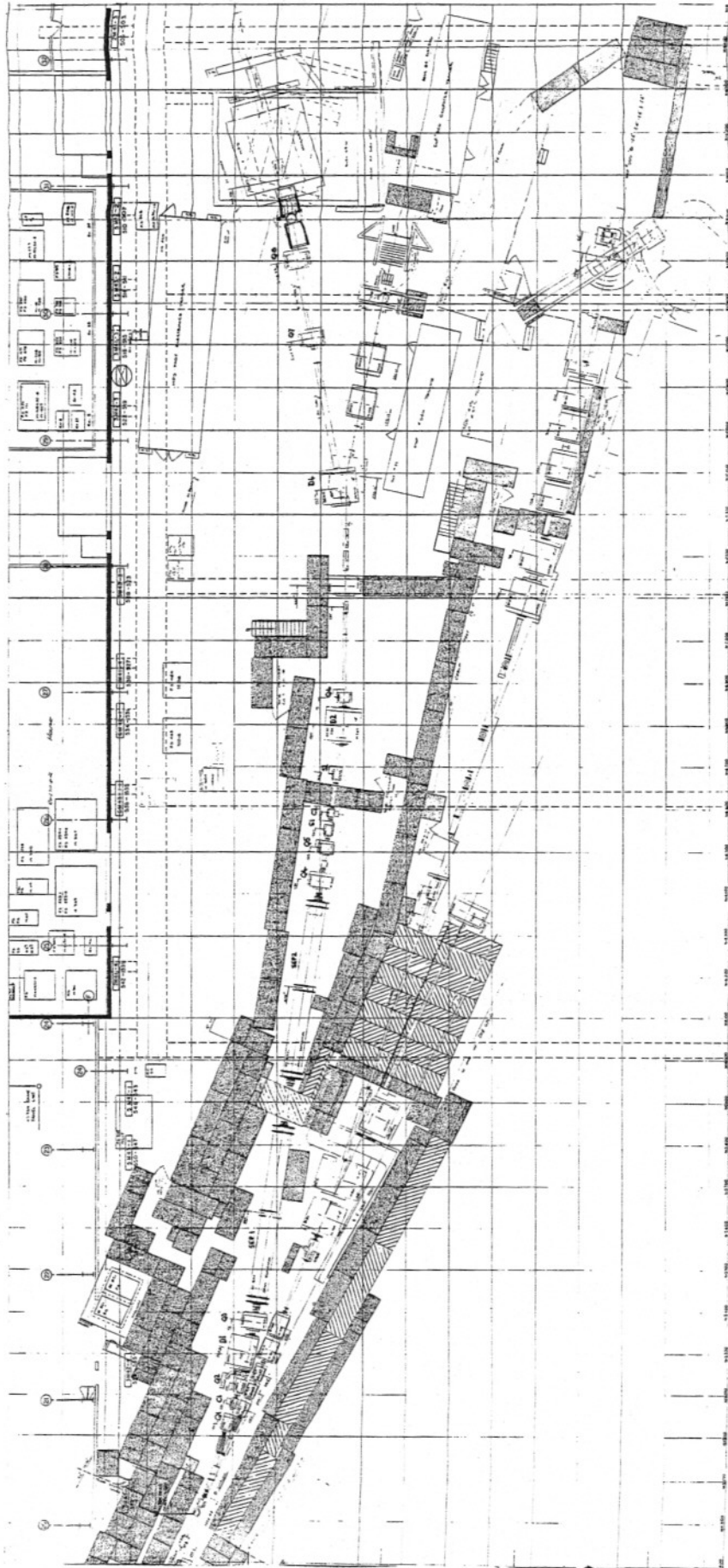
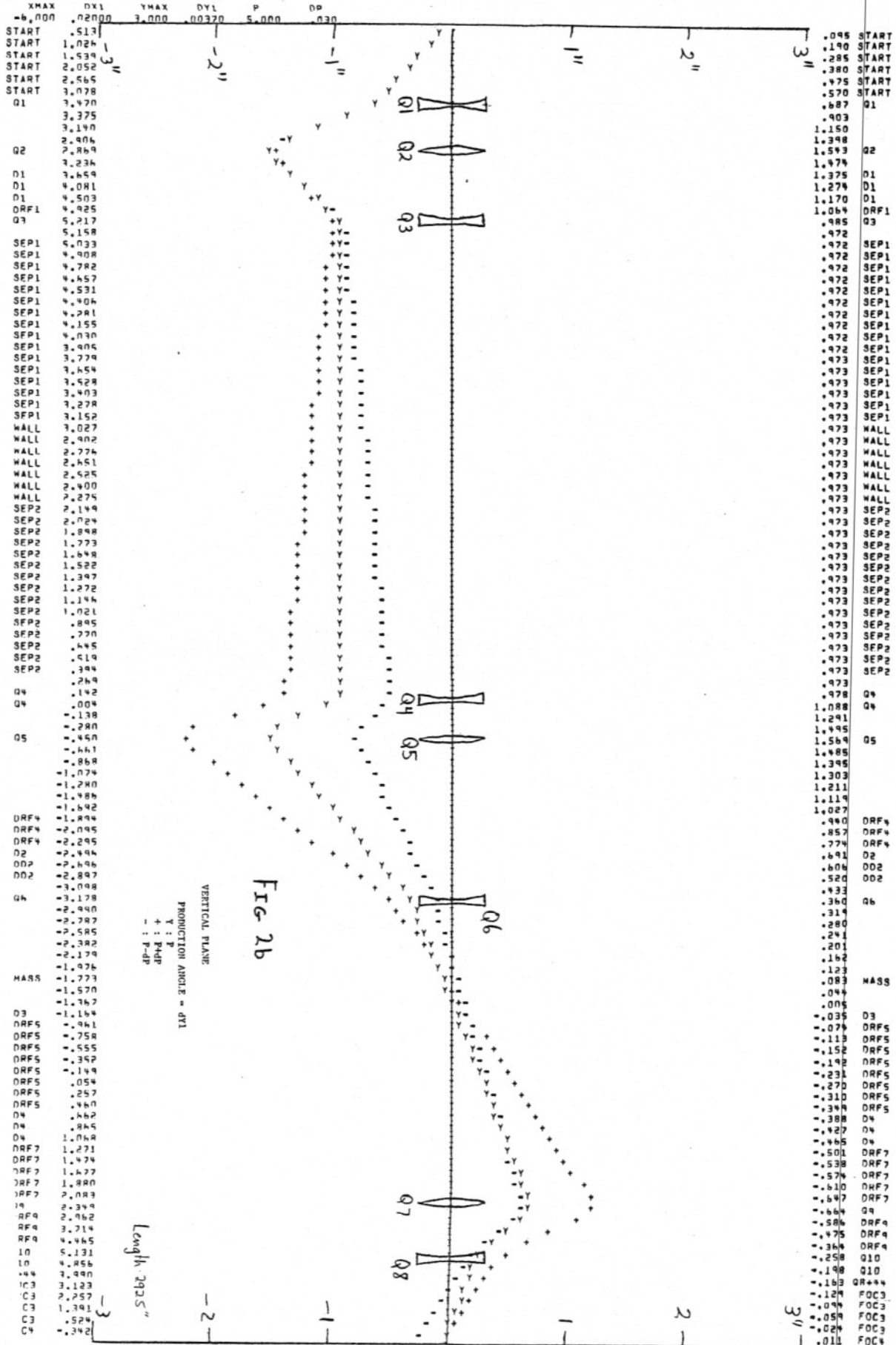


Figure 1



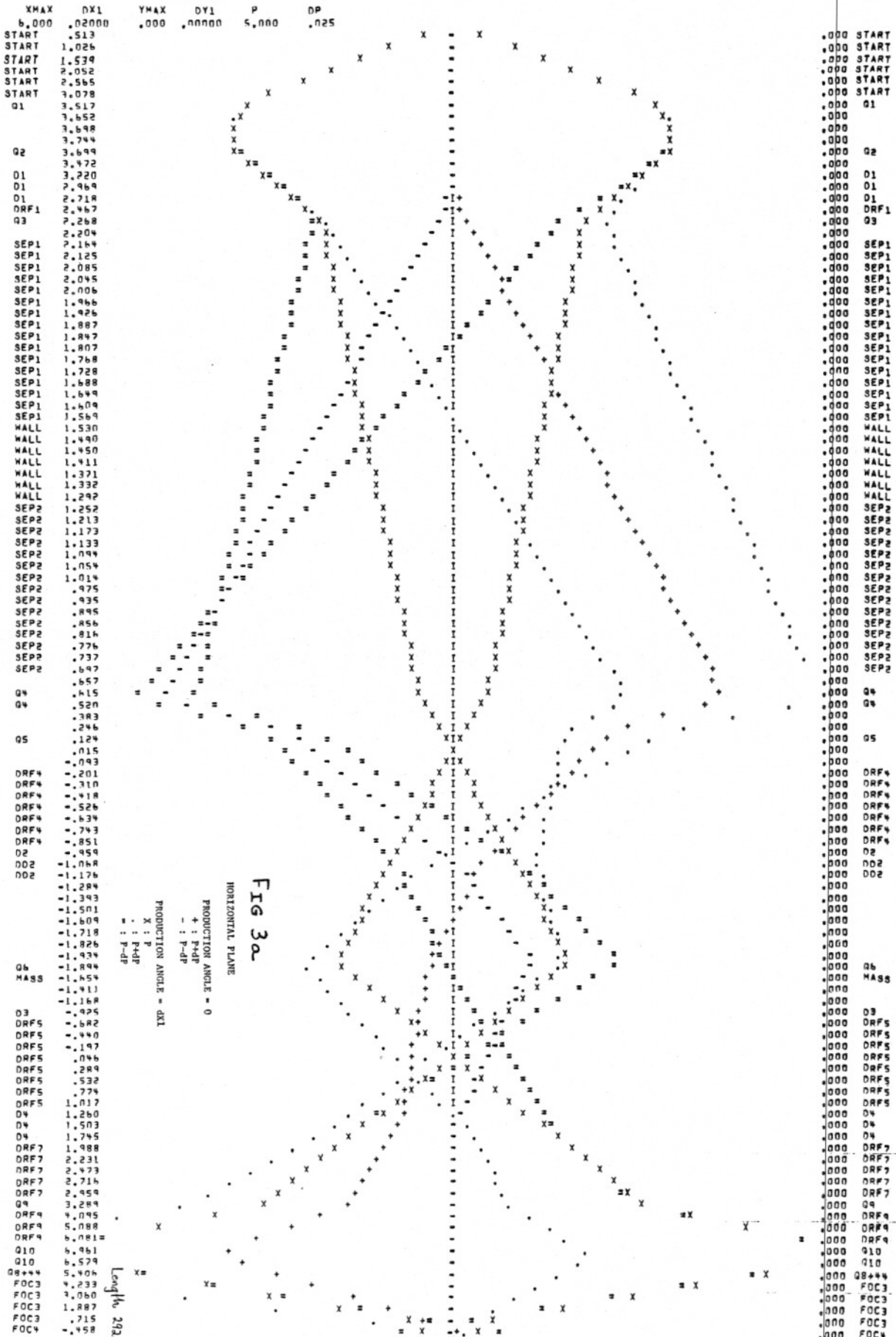


Fig 3a

HORIZONTAL PLANE
 PRODUCTION ANGLE = 0
 + : P+P
 - : P-P
 PRODUCTION ANGLE = DX1
 X : P
 + : P+P
 - : P-P

Length 2925"

XMAX	DY1	YMAX	DY1	P	DP
46.000	.02000	3.000	.00320	5.000	.030
START	.570				
START	1.139				
START	1.709				
START	2.279				
START	2.849				
Q1	3.419				
	3.989				
	4.559				
Q2	5.129				
	5.699				
O1	6.269				
O1	6.839				
DRF1	7.409				
Q3	7.979				
	8.549				
SEP1	9.119				
SEP1	9.689				
SEP1	10.259				
SEP1	10.829				
SEP1	11.399				
SEP1	11.969				
SEP1	12.539				
SEP1	13.109				
SEP1	13.679				
SEP1	14.249				
SEP1	14.819				
SEP1	15.389				
SEP1	15.959				
SEP1	16.529				
SEP1	17.099				
SEP1	17.669				
SEP1	18.239				
SEP1	18.809				
SEP1	19.379				
SEP1	19.949				
SEP1	20.519				
SEP1	21.089				
SEP1	21.659				
SEP1	22.229				
SEP1	22.799				
SEP1	23.369				
SEP1	23.939				
SEP1	24.509				
SEP1	25.079				
SEP1	25.649				
SEP1	26.219				
SEP1	26.789				
SEP1	27.359				
SEP1	27.929				
SEP1	28.499				
SEP1	29.069				
SEP1	29.639				
SEP1	30.209				
SEP1	30.779				
SEP1	31.349				
SEP1	31.919				
SEP1	32.489				
SEP1	33.059				
SEP1	33.629				
SEP1	34.199				
SEP1	34.769				
SEP1	35.339				
SEP1	35.909				
SEP1	36.479				
SEP1	37.049				
SEP1	37.619				
SEP1	38.189				
SEP1	38.759				
SEP1	39.329				
SEP1	39.899				
SEP1	40.469				
SEP1	41.039				
SEP1	41.609				
SEP1	42.179				
SEP1	42.749				
SEP1	43.319				
SEP1	43.889				
SEP1	44.459				
SEP1	45.029				
SEP1	45.599				
SEP1	46.169				
SEP1	46.739				
SEP1	47.309				
SEP1	47.879				
SEP1	48.449				
SEP1	49.019				
SEP1	49.589				
SEP1	50.159				
SEP1	50.729				
SEP1	51.299				
SEP1	51.869				
SEP1	52.439				
SEP1	53.009				
SEP1	53.579				
SEP1	54.149				
SEP1	54.719				
SEP1	55.289				
SEP1	55.859				
SEP1	56.429				
SEP1	56.999				
SEP1	57.569				
SEP1	58.139				
SEP1	58.709				
SEP1	59.279				
SEP1	59.849				
SEP1	60.419				
SEP1	60.989				
SEP1	61.559				
SEP1	62.129				
SEP1	62.699				
SEP1	63.269				
SEP1	63.839				
SEP1	64.409				
SEP1	64.979				
SEP1	65.549				
SEP1	66.119				
SEP1	66.689				
SEP1	67.259				
SEP1	67.829				
SEP1	68.399				
SEP1	68.969				
SEP1	69.539				
SEP1	70.109				
SEP1	70.679				
SEP1	71.249				
SEP1	71.819				
SEP1	72.389				
SEP1	72.959				
SEP1	73.529				
SEP1	74.099				
SEP1	74.669				
SEP1	75.239				
SEP1	75.809				
SEP1	76.379				
SEP1	76.949				
SEP1	77.519				
SEP1	78.089				
SEP1	78.659				
SEP1	79.229				
SEP1	79.799				
SEP1	80.369				
SEP1	80.939				
SEP1	81.509				
SEP1	82.079				
SEP1	82.649				
SEP1	83.219				
SEP1	83.789				
SEP1	84.359				
SEP1	84.929				
SEP1	85.499				
SEP1	86.069				
SEP1	86.639				
SEP1	87.209				
SEP1	87.779				
SEP1	88.349				
SEP1	88.919				
SEP1	89.489				
SEP1	90.059				
SEP1	90.629				
SEP1	91.199				
SEP1	91.769				
SEP1	92.339				
SEP1	92.909				
SEP1	93.479				
SEP1	94.049				
SEP1	94.619				
SEP1	95.189				
SEP1	95.759				
SEP1	96.329				
SEP1	96.899				
SEP1	97.469				
SEP1	98.039				
SEP1	98.609				
SEP1	99.179				
SEP1	99.749				
SEP1	100.319				
SEP1	100.889				
SEP1	101.459				
SEP1	102.029				
SEP1	102.599				
SEP1	103.169				
SEP1	103.739				
SEP1	104.309				
SEP1	104.879				
SEP1	105.449				
SEP1	106.019				
SEP1	106.589				
SEP1	107.159				
SEP1	107.729				
SEP1	108.299				
SEP1	108.869				
SEP1	109.439				
SEP1	110.009				
SEP1	110.579				
SEP1	111.149				
SEP1	111.719				
SEP1	112.289				
SEP1	112.859				
SEP1	113.429				
SEP1	113.999				
SEP1	114.569				
SEP1	115.139				
SEP1	115.709				
SEP1	116.279				
SEP1	116.849				
SEP1	117.419				
SEP1	117.989				
SEP1	118.559				
SEP1	119.129				
SEP1	119.699				
SEP1	120.269				
SEP1	120.839				
SEP1	121.409				
SEP1	121.979				
SEP1	122.549				
SEP1	123.119				
SEP1	123.689				
SEP1	124.259				
SEP1	124.829				
SEP1	125.399				
SEP1	125.969				
SEP1	126.539				
SEP1	127.109				
SEP1	127.679				
SEP1	128.249				
SEP1	128.819				
SEP1	129.389				
SEP1	129.959				
SEP1	130.529				
SEP1	131.099				
SEP1	131.669				
SEP1	132.239				
SEP1	132.809				
SEP1	133.379				
SEP1	133.949				
SEP1	134.519				
SEP1	135.089				
SEP1	135.659				
SEP1	136.229				
SEP1	136.799				
SEP1	137.369				
SEP1	137.939				
SEP1	138.509				
SEP1	139.079				
SEP1	139.649				
SEP1	140.219				
SEP1	140.789				
SEP1	141.359				
SEP1	141.929				
SEP1	142.499				
SEP1	143.069				
SEP1	143.639				
SEP1	144.209				
SEP1	144.779				
SEP1	145.349				
SEP1	145.919				
SEP1	146.489				
SEP1	147.059				
SEP1	147.629				
SEP1	148.199				
SEP1	148.769				
SEP1	149.339				
SEP1	149.909				
SEP1	150.479				
SEP1	151.049				
SEP1	151.619				
SEP1	152.189				
SEP1	152.759				
SEP1	153.329				
SEP1	153.899				
SEP1	154.469				
SEP1	155.039				
SEP1	155.609				
SEP1	156.179				
SEP1	156.749				
SEP1	157.319				
SEP1	157.889				
SEP1	158.459				
SEP1	159.029				
SEP1	159.599				
SEP1	160.169				
SEP1	160.739				
SEP1	161.309				
SEP1	161.879				
SEP1	162.449				
SEP1	163.019				
SEP1	163.589				
SEP1	164.159				
SEP1	164.729				
SEP1	165.299				
SEP1	165.869				
SEP1	166.439				
SEP1	167.009				
SEP1	167.579				
SEP1	168.149				
SEP1	168.719				
SEP1	169.289				
SEP1	169.859				
SEP1	170.429				
SEP1	170.999				
SEP1	171.569				
SEP1	172.139				
SEP1	172.709				
SEP1	173.279				
SEP1	173.849				
SEP1	174.419				
SEP1	174.989				
SEP1	175.559				
SEP1	176.129				

XMAX	DX1	YMAX	DY1	P	DP			
-6.000	.02000	3.000	.00115	5.000	.025			
START	.566					YI	.033	START
START	1.132					YI	.065	START
START	1.698					YI	.098	START
START	2.264					YI	.130	START
START	2.830					YI	.163	START
Q1	3.396					YI	.196	Q1
	3.439					YI	.247	
	3.640					YI	.311	
	3.741					YI	.375	
Q2	3.694					YI	.444	Q2
	3.434					YI	.514	
D1	3.156					YI	.651	D1
D1	2.877					YI	.752	D1
D1	2.598					YI	.851	D1
Q3	2.330					YI	.944	Q3
	2.204					YI	.978	
SEP1	2.157					YI	.978	SEP1
SEP1	2.110					YI	.978	SEP1
SFP1	2.063					YI	.978	SEP1
SEP1	2.015					YI	.978	SEP1
SEP1	1.968					YI	.978	SEP1
SFP1	1.921					YI	.978	SEP1
SEP1	1.874					YI	.978	SEP1
SEP1	1.826					YI	.978	SEP1
SEP1	1.779					YI	.978	SEP1
SEP1	1.732					YI	.978	SEP1
SEP1	1.685					YI	.978	SEP1
SEP1	1.638					YI	.978	SEP1
SEP1	1.590					YI	.978	SEP1
SFP1	1.543					YI	.978	SEP1
SFP1	1.496					YI	.978	SEP1
WALL	1.449					YI	.978	WALL
WALL	1.401					YI	.978	WALL
WALL	1.354					YI	.978	WALL
WALL	1.307					YI	.978	WALL
WALL	1.260					YI	.978	WALL
WALL	1.212					YI	.978	WALL
SEP2	1.165					YI	.978	WALL
SEP2	1.118					YI	.978	WALL
SEP2	1.071					YI	.978	WALL
SEP2	1.024					YI	.978	WALL
SEP2	.976					YI	.978	WALL
SEP2	.929					YI	.978	WALL
SEP2	.882					YI	.978	WALL
SEP2	.835					YI	.978	WALL
SEP2	.787					YI	.978	WALL
SEP2	.740					YI	.978	WALL
SEP2	.693					YI	.978	WALL
SEP2	.646					YI	.978	WALL
SEP2	.599					YI	.978	WALL
SEP2	.551					YI	.978	WALL
SEP2	.504					YI	.978	WALL
Q4	.444					YI	.978	WALL
DRF2	.340					YI	.978	WALL
DRF2	.274					YI	.978	WALL
Q5	.114					YI	.978	WALL
SEX1	.024					YI	.978	WALL
	-0.062					YI	.978	WALL
	-0.151					YI	.978	WALL
SEX2	-0.241					YI	.978	WALL
SEX2	-0.330					YI	.978	WALL
DRF3	-0.420					YI	.978	WALL
DRF3	-0.509					YI	.978	WALL
DRF3	-0.598					YI	.978	WALL
D2	-0.688					YI	.978	WALL
D2	-0.777					YI	.978	WALL
DD2	-0.867					YI	.978	WALL
	-0.956					YI	.978	WALL
Q6	-1.017					YI	.978	WALL
	-1.027					YI	.978	WALL
	-1.035					YI	.978	WALL
	-1.044					YI	.978	WALL
	-1.053					YI	.978	WALL
	-1.061					YI	.978	WALL
MASS	-1.070					YI	.978	WALL
MASS	-1.079					YI	.978	WALL
	-1.087					YI	.978	WALL
	-1.095					YI	.978	WALL
D3	-1.104					YI	.978	WALL
DRF5	-1.112					YI	.978	WALL
DRF5	-1.121					YI	.978	WALL
DRF5	-1.124					YI	.978	WALL
DRF5	-1.134					YI	.978	WALL
DRF5	-1.147					YI	.978	WALL
DRF5	-1.155					YI	.978	WALL
D4	-1.164					YI	.978	WALL
D4	-1.172					YI	.978	WALL
DRF7	-1.181					YI	.978	WALL
DRF7	-1.189					YI	.978	WALL
DRF7	-1.198					YI	.978	WALL
DRF7	-1.206					YI	.978	WALL
DRF7	-1.215					YI	.978	WALL
DRF7	-1.223					YI	.978	WALL
DRF7	-1.232					YI	.978	WALL
DRF7	-1.240					YI	.978	WALL
DRF7	-1.249					YI	.978	WALL
DRF7	-1.258					YI	.978	WALL
DRF7	-1.266					YI	.978	WALL
Q7	-1.328					YI	.978	WALL
DRF9	-1.524					YI	.978	WALL
DRF9	-1.736					YI	.978	WALL
DRF9	-1.948					YI	.978	WALL
DRF9	-2.161					YI	.978	WALL
DRF9	-2.373					YI	.978	WALL
Q8	-2.577					YI	.978	WALL
Q8	-2.449					YI	.978	WALL
Q8+44	-2.045					YI	.978	WALL
FOC2	-1.719					YI	.978	WALL
FOC2	-1.344					YI	.978	WALL
FOC2	-1.168					YI	.978	WALL
FOC2	-0.933					YI	.978	WALL
FOC2	-0.717					YI	.978	WALL
FOC3	-0.518					YI	.978	WALL
ESS	.055					YI	.978	WALL

FIG 5B

VERTICAL PLANE
 Y : Y
 + : PMP
 - : P-MP
 PRODUCTION ANGLE = DTI

Length 3200"

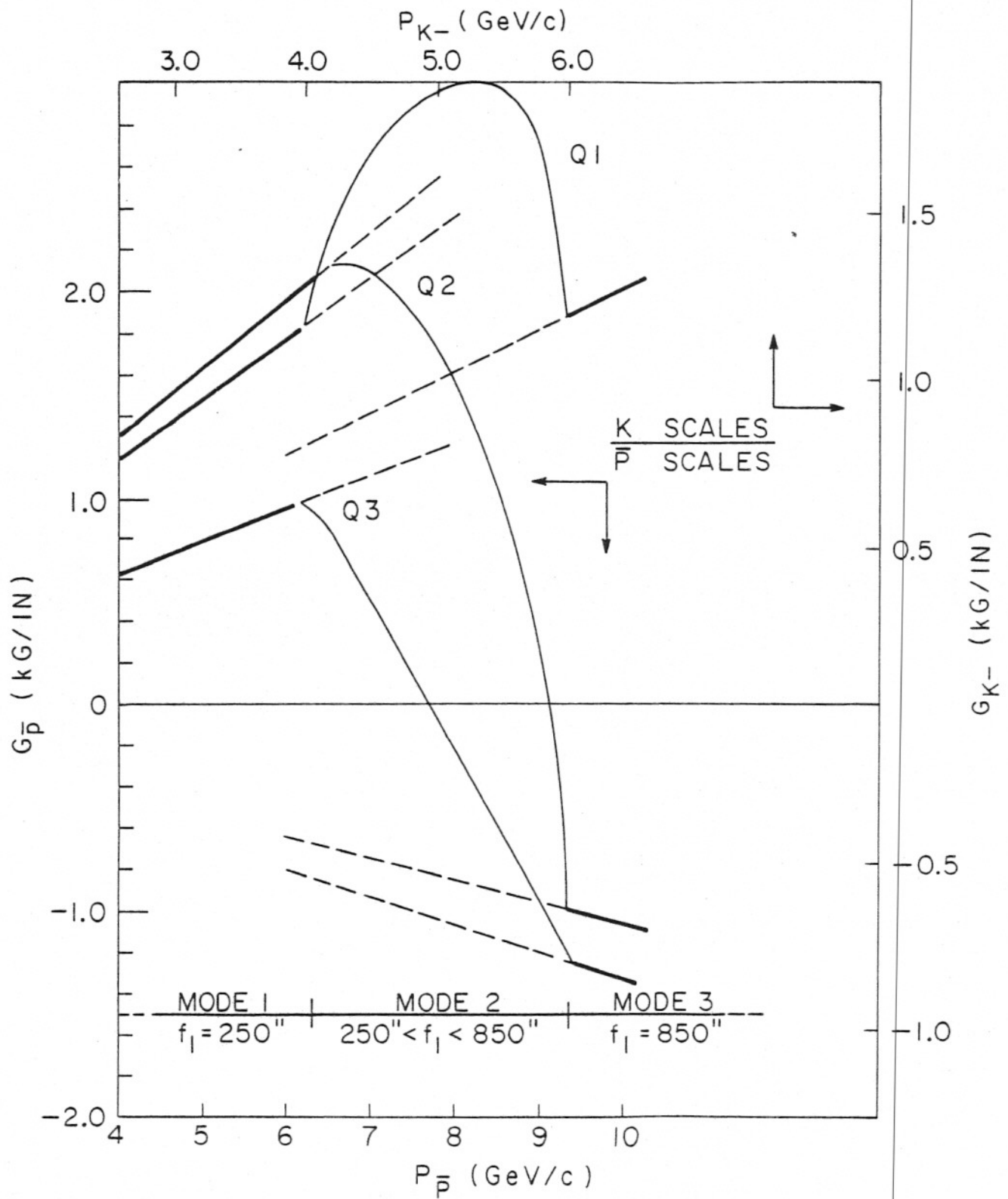


Figure 7

XMAX	DX1	YMAX	OY1	P	DP
-4.000	.02000	3.000	.00115	5.000	.015
START	1.566				
START	1.132				
START	1.698				
START	2.264				
START	2.830				
Q1	3.381				
	3.639				
	3.640				
	3.741				
Q2	3.642				
	3.429				
D1	3.145				
D1	2.860				
D1	2.576				
Q3	2.302				
	2.170				
SEP1	2.115				
SEP1	2.060				
SEP1	2.005				
SFP1	1.950				
SEP1	1.895				
SEP1	1.840				
SEP1	1.785				
SEP1	1.730				
SEP1	1.675				
SEP1	1.621				
SEP1	1.566				
SEP1	1.511				
SEP1	1.456				
SEP1	1.401				
SFP1	1.346				
WALL	1.291				
WALL	1.236				
WALL	1.181				
WALL	1.126				
WALL	1.072				
WALL	1.017				
SEP2	.962				
SEP2	.907				
SEP2	.852				
SEP2	.797				
SEP2	.742				
SEP2	.687				
SEP2	.632				
SEP2	.577				
SEP2	.522				
SEP2	.468				
SFP2	.413				
SFP2	.358				
SEP2	.303				
SEP2	.248				
	.193				
Q4	.142				
DRF2	.105				
DRF3	.070				
Q5	.033				
	-.004				
	-.050				
DR64	-.092				
DR64	-.133				
DR64	-.174				
DR64	-.216				
DR64	-.257				
DRF3	-.298				
D2	-.340				
D2	-.381				
NO2	-.422				
	-.464				
Q6	-.506				
DRF4	-.551				
DRF4	-.596				
	-.641				
	-.686				
	-.732				
	-.777				
HASP	-.822				
	-.867				
D3	-.912				
DRF5	-.957				
DRF5	-1.002				
DRF5	-1.047				
DRF5	-1.092				
DRF5	-1.137				
DRF5	-1.182				
DRF5	-1.227				
OD4	-1.272				
U4	-1.317				
DRF7	-1.362				
DRF7	-1.407				
DRF7	-1.452				
DRF7	-1.497				
DRF7	-1.542				
DRF7	-1.587				
DRF7	-1.632				
DRF7	-1.677				
DRF7	-1.722				
DRF7	-1.767				
DRF7	-1.812				
Q4	-1.857				
DRF9	-1.902				
DRF9	-1.947				
Q10	-1.992				
Q10	-2.037				
Q10	-2.082				
Q10	-2.127				
Q10	-2.172				
Q10	-2.217				
Q10	-2.262				
Q10	-2.307				
Q10	-2.352				
Q10	-2.397				
Q10	-2.442				
Q10	-2.487				
Q10	-2.532				
Q10	-2.577				
Q10	-2.622				
Q10	-2.667				
Q10	-2.712				
Q10	-2.757				
Q10	-2.802				
Q10	-2.847				
Q10	-2.892				
Q10	-2.937				
Q10	-2.982				
Q10	-3.027				
Q10	-3.072				
Q10	-3.117				
Q10	-3.162				
Q10	-3.207				
Q10	-3.252				
Q10	-3.297				
Q10	-3.342				
Q10	-3.387				
Q10	-3.432				
Q10	-3.477				
Q10	-3.522				
Q10	-3.567				
Q10	-3.612				
Q10	-3.657				
Q10	-3.702				
Q10	-3.747				
Q10	-3.792				
Q10	-3.837				
Q10	-3.882				
Q10	-3.927				
Q10	-3.972				
Q10	-4.017				
Q10	-4.062				
Q10	-4.107				
Q10	-4.152				
Q10	-4.197				
Q10	-4.242				
Q10	-4.287				
Q10	-4.332				
Q10	-4.377				
Q10	-4.422				
Q10	-4.467				
Q10	-4.512				
Q10	-4.557				
Q10	-4.602				
Q10	-4.647				
Q10	-4.692				
Q10	-4.737				
Q10	-4.782				
Q10	-4.827				
Q10	-4.872				
Q10	-4.917				
Q10	-4.962				
Q10	-5.007				
Q10	-5.052				
Q10	-5.097				
Q10	-5.142				
Q10	-5.187				
Q10	-5.232				
Q10	-5.277				
Q10	-5.322				
Q10	-5.367				
Q10	-5.412				
Q10	-5.457				
Q10	-5.502				
Q10	-5.547				
Q10	-5.592				
Q10	-5.637				
Q10	-5.682				
Q10	-5.727				
Q10	-5.772				
Q10	-5.817				
Q10	-5.862				
Q10	-5.907				
Q10	-5.952				
Q10	-5.997				
Q10	-6.042				
Q10	-6.087				
Q10	-6.132				
Q10	-6.177				
Q10	-6.222				
Q10	-6.267				
Q10	-6.312				
Q10	-6.357				
Q10	-6.402				
Q10	-6.447				
Q10	-6.492				
Q10	-6.537				
Q10	-6.582				
Q10	-6.627				
Q10	-6.672				
Q10	-6.717				
Q10	-6.762				
Q10	-6.807				
Q10	-6.852				
Q10	-6.897				
Q10	-6.942				
Q10	-6.987				
Q10	-7.032				
Q10	-7.077				
Q10	-7.122				
Q10	-7.167				
Q10	-7.212				
Q10	-7.257				
Q10	-7.302				
Q10	-7.347				
Q10	-7.392				
Q10	-7.437				
Q10	-7.482				
Q10	-7.527				
Q10	-7.572				
Q10	-7.617				
Q10	-7.662				
Q10	-7.707				
Q10	-7.752				
Q10	-7.797				
Q10	-7.842				
Q10	-7.887				
Q10	-7.932				
Q10	-7.977				
Q10	-8.022				
Q10	-8.067				
Q10	-8.112				
Q10	-8.157				
Q10	-8.202				
Q10	-8.247				
Q10	-8.292				
Q10	-8.337				
Q10	-8.382				
Q10	-8.427				
Q10	-8.472				
Q10	-8.517				
Q10	-8.562				
Q10	-8.607				
Q10	-8.652				
Q10	-8.697				
Q10	-8.742				
Q10	-8.787				
Q10	-8.832				
Q10	-8.877				
Q10	-8.922				
Q10	-8.967				
Q10	-9.012				
Q10	-9.057				
Q10	-9.102				
Q10	-9.147				
Q10	-9.192				
Q10	-9.237				
Q10	-9.282				
Q10	-9.327				
Q10	-9.372				
Q10	-9.417				
Q10	-9.462				
Q10	-9.507				
Q10	-9.552				
Q10	-9.597				
Q10	-9.642				
Q10	-9.687				
Q10	-9.732				
Q10	-9.777				
Q10	-9.822				
Q10	-9.867				
Q10	-9.912				
Q10	-9.957				
Q10	-10.002				
Q10	-10.047				
Q10	-10.092				
Q10	-10.137				
Q10	-10.182				
Q10	-10.227				
Q10	-10.272				
Q10	-10.317				
Q10	-10.362				
Q10	-10.407				
Q10	-10.452				
Q10	-10.497				
Q10	-10.542				
Q10	-10.587				
Q10	-10.632				
Q10	-10.677				
Q10	-10.722				
Q10	-10.767				
Q10	-10.812				
Q10	-10.857				
Q10	-10.902				
Q10	-10.947				
Q10	-10.992				
Q10	-11.037				
Q10	-11.082				
Q10	-11.127				
Q10	-11.172				
Q10	-11.217				
Q10	-11.262				
Q10	-11.307				
Q10	-11.352				
Q10	-11.397				
Q10	-11.442				
Q10	-11.487				
Q10	-11.532				
Q10	-11.577				

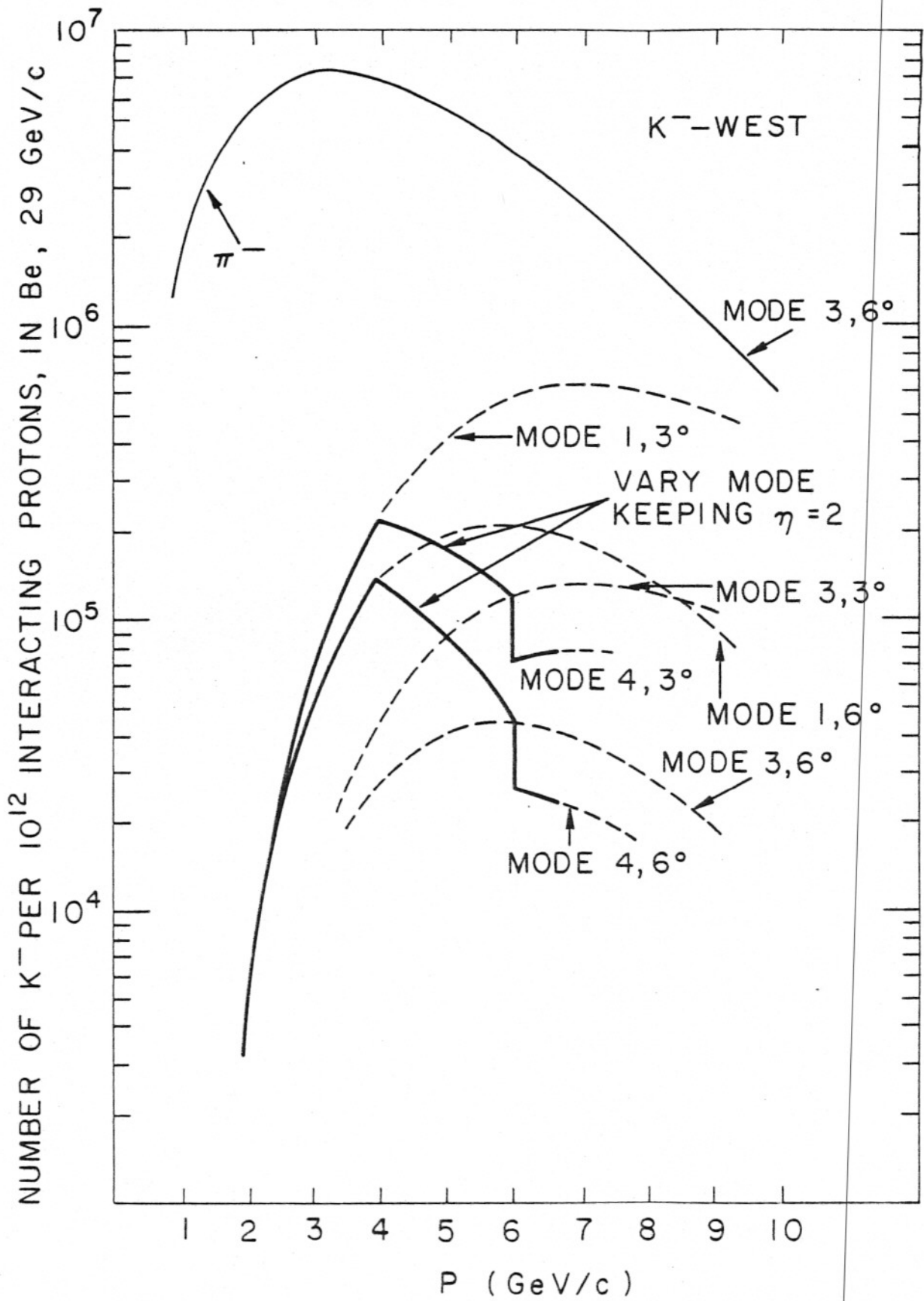


Figure 8

NUMBER OF K^+ PER 10^{12} INTERACTING PROTONS, IN Be, 29 GeV/c

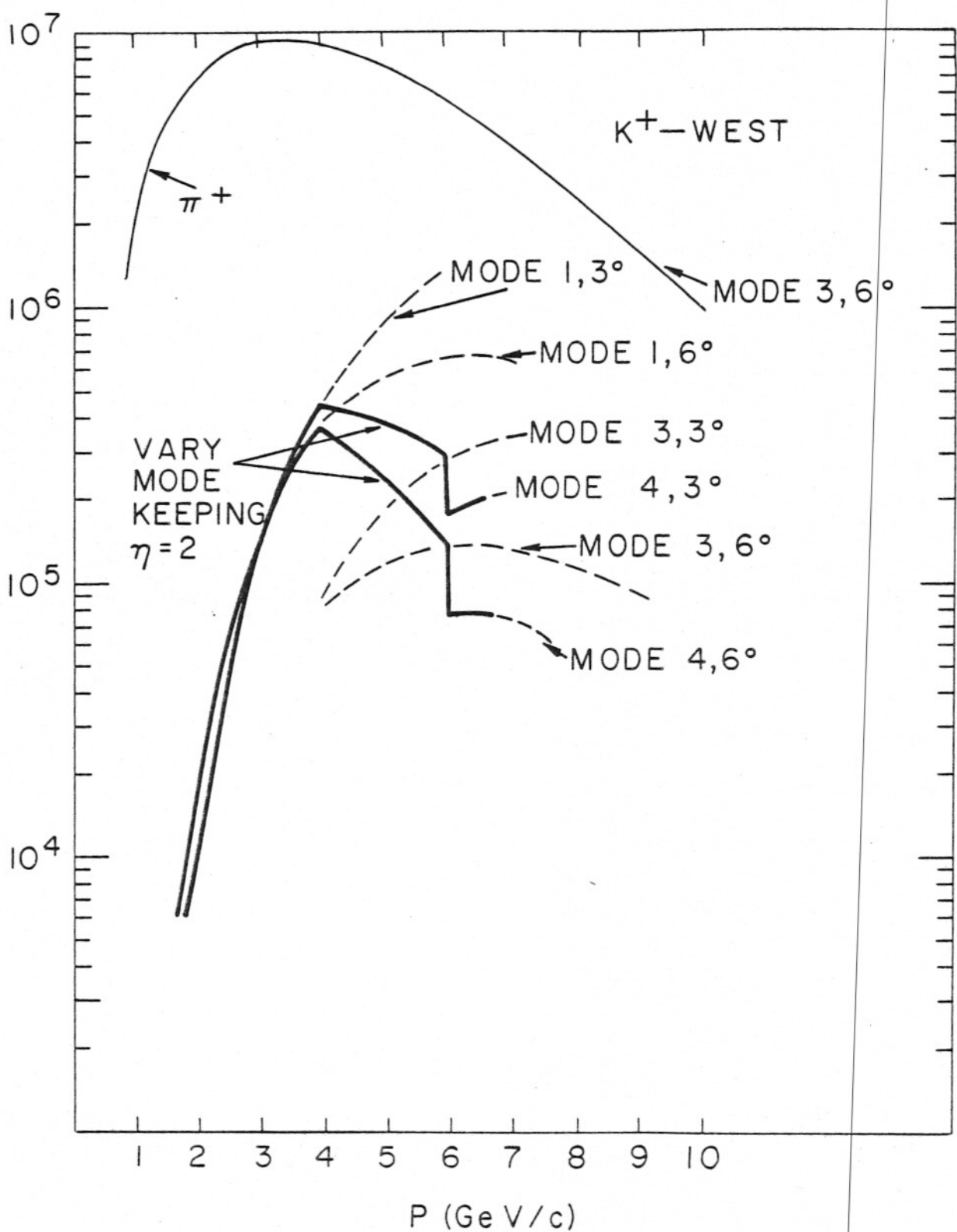


Figure 9

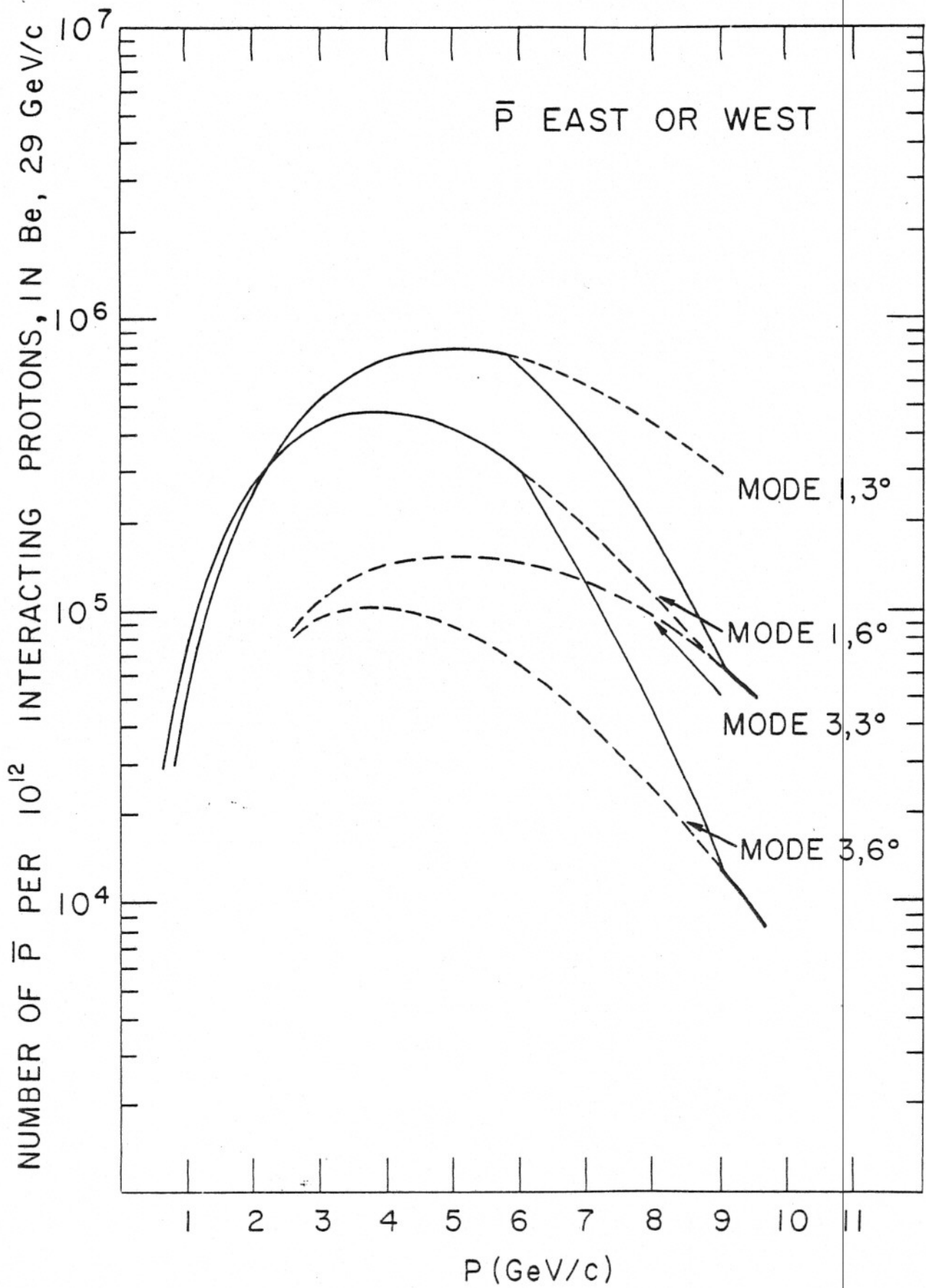


Figure 10

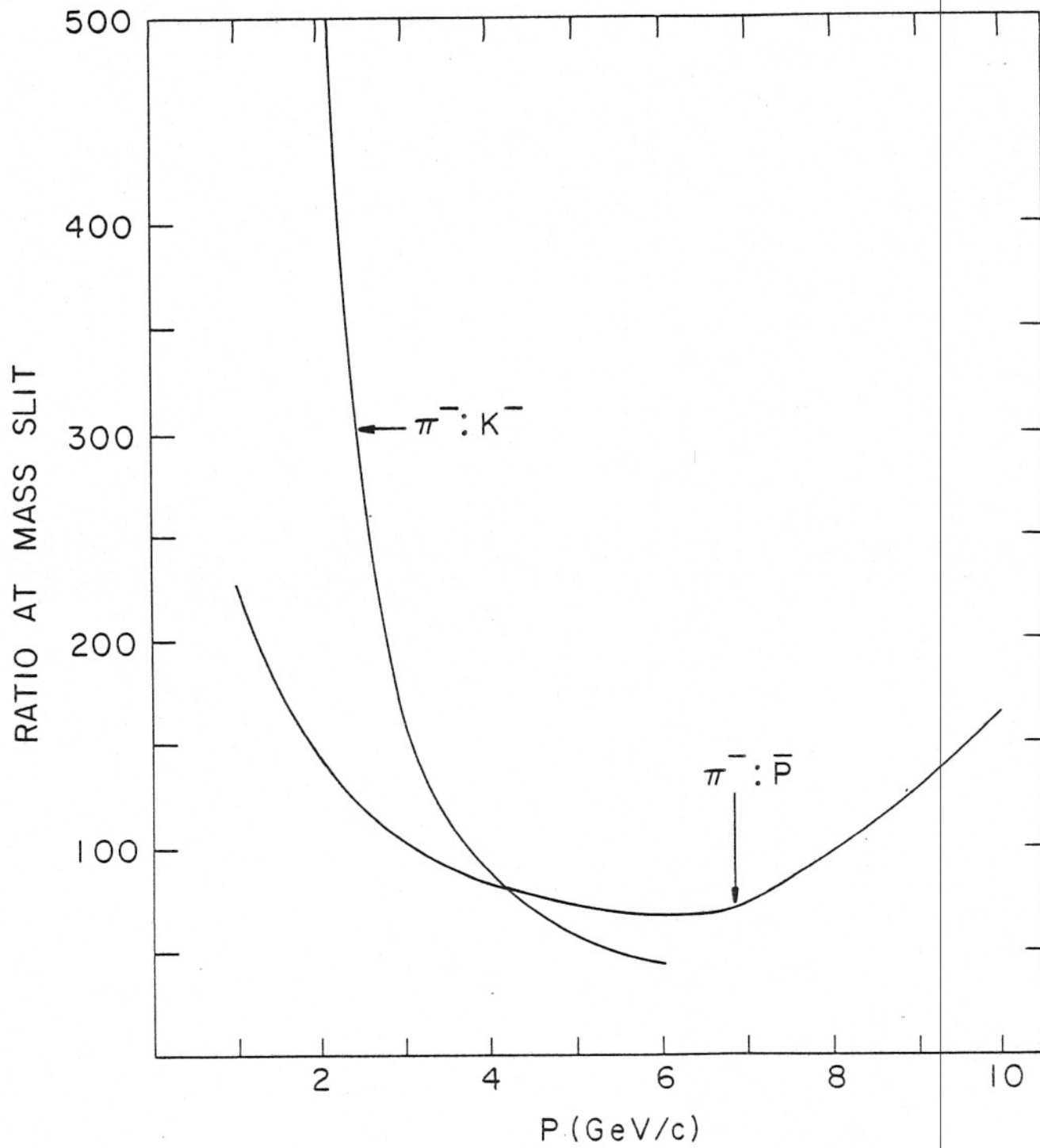


Figure 11

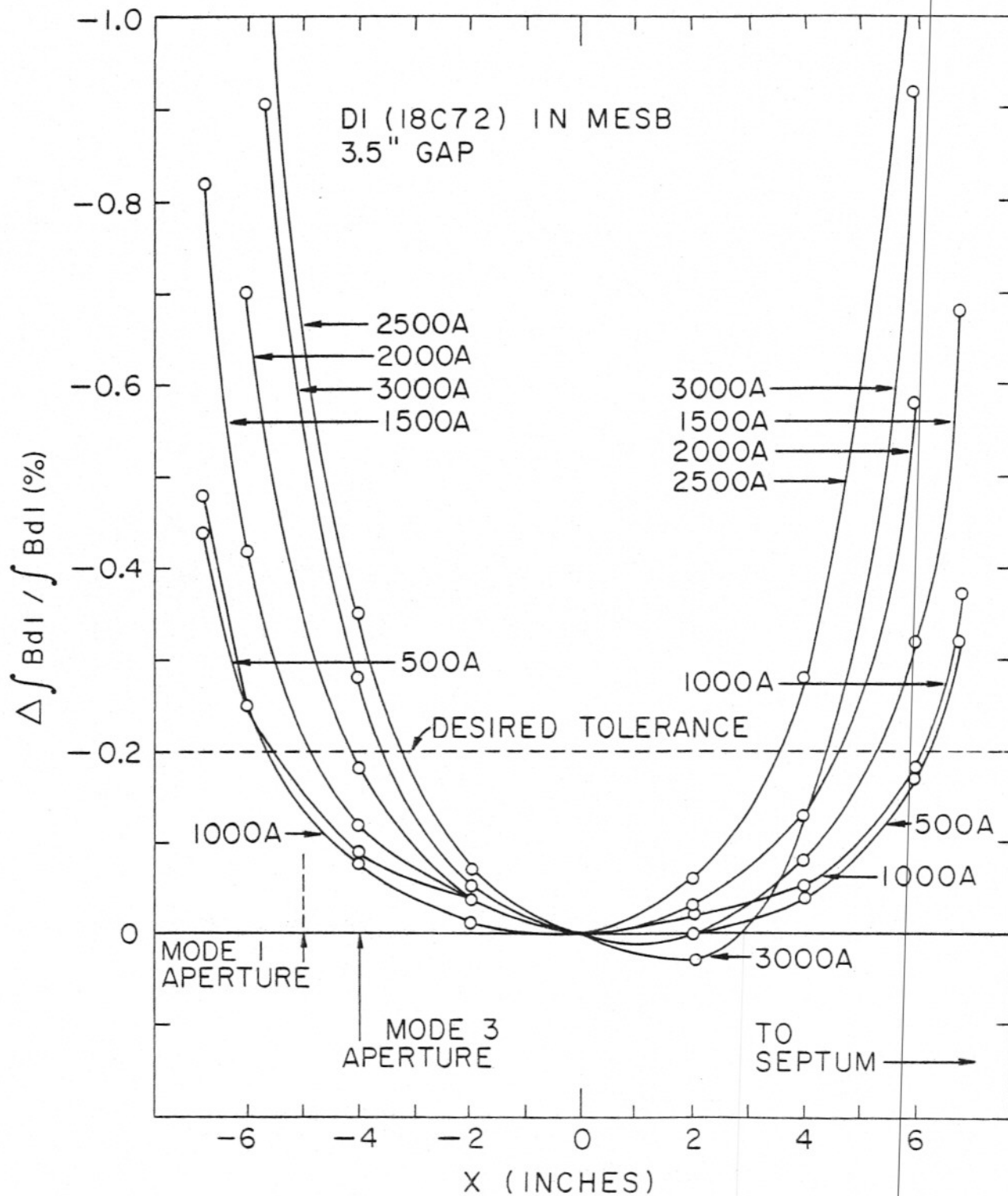


Figure 12

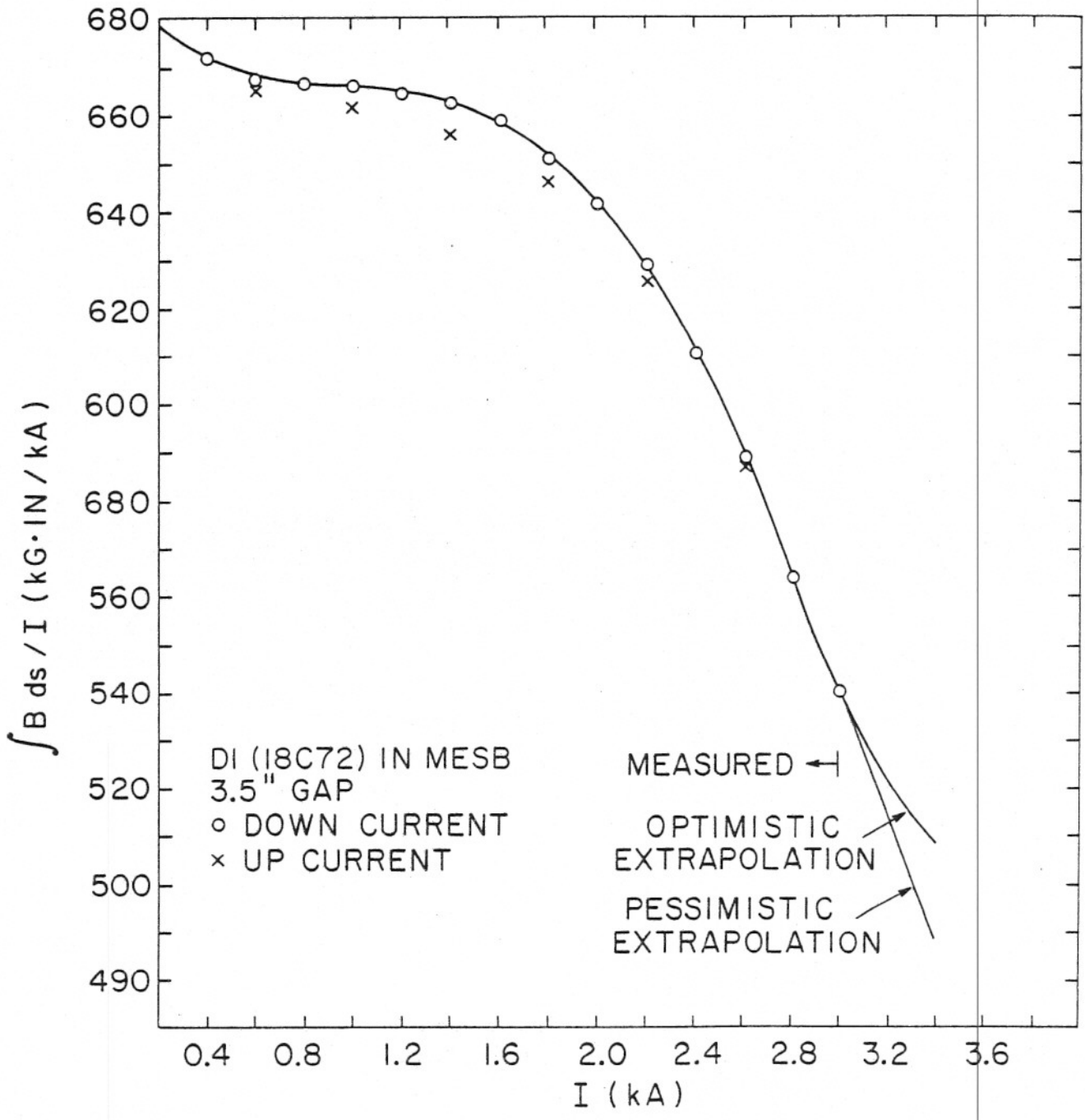


Figure 13

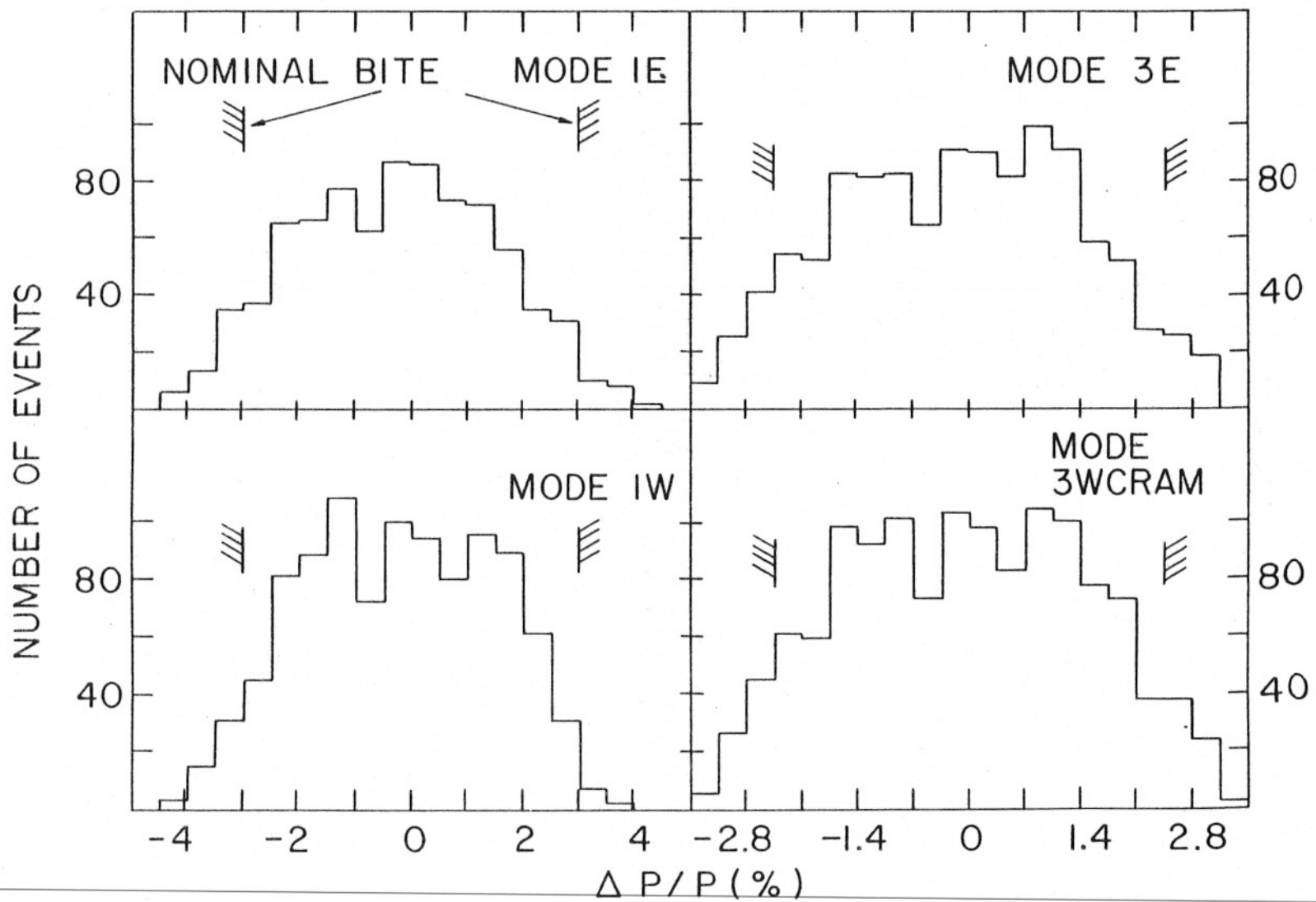


Figure 14

Appendix II-B1

The beam is of conventional design. Particles produced at 0° are focused by a doublet and momentum dispersed at slit located at the approximate mid-point of the channel. The second half of the beam is almost a reflection of the first; momenta are re-combined, and a second doublet brings the particles to their final focus.

Five quadrupoles form the upstream doublet. First, three N8Q32s focus vertically, then two 8Q48s horizontally. The beam is momentum dispersed at a slit located 700" from the production target by a 4.1° bend in two 18D72s. The second bend is also 4.1° in two 18D72s, and the second doublet consists of two 12Q60s focusing horizontally, then two vertically.

There are two collimators in the beam. B1C1 lies ahead of the first dipole and intercepts the diffracted protons. When narrowed, the slit walls can produce secondary particles, so this collimator cannot be used as an effective intensity limiter. B1C2 (the momentum slit) has remotely controlled horizontal and vertical apertures.

The beam has performed close to its design criteria. Table I gives some of its parameters, and Table II gives the currents, shunt readings, and Dybbuk set points for 20 GeV/c. Other operating points can be obtained by scaling.

Table I Beam Parameters

Vertical Acceptance	± 16 mrad
Horizontal Acceptance	± 4.8 mrad
Magnification at 2nd Focus	1.5 (V) x 1.3 (H)
Dispersion at Momentum Slit	1.6%/inch

Table II

B1 - 20 GeV/c Negative Beam

	<u>Type</u>	<u>Current (Polarity)</u>	<u>Field or Gradient</u>	<u>Dybbuk</u>
Q1	N8Q32	1913 (A)	2.225	1913
Q2	N8Q32	1913 (A)	2.225	1913
Q3	N8Q32	1913 (A)	2.225	1913
Q4	8Q48	1304 (B)	1.683	2086
Q5	8Q48	1304 (B)	1.683	2086
D1	18D72	1508 (B)	13.91	1508
D2	18D72	1508 (B)	13.91	1508
D3	18D72	1508 (B)	13.91	1508
D4	18D72	1508 (B)	13.91	1508
Q6	12Q60	995 (B)	0.830	1592
Q7	12Q60	995 (B)	0.830	1592
Q8	12Q60	961 (A)	0.803	1538
Q9	12Q60	961 (A)	0.803	961

Note: Dybbuk set points do not necessarily correspond to currents.